Received: 31 March 2018 | Revised: 14 January 2019 | Accepted: 1 February 2019

DOI: 10.1002/wsbm.1447

WIREs SYSTEMS BIOLOGY AND MEDICINE WILEY

OVERVIEW

IL7 receptor signaling in T cells: A mathematical modeling perspective

Jung-Hyun Park[1] | Adam T. Waickman[1] | Joseph Reynolds[2] | Mario Castro[3,4] | Carmen Molina-París[4]

[1]Experimental Immunology Branch, National Cancer Institute, NIH, Bethesda, Maryland

[2]Safety and Environmental Assurance Centre (SEAC), Unilever, UK

[3]Universidad Pontificia Comillas, GISC and DNL, Madrid, Spain

[4]Department of Applied Mathematics, School of Mathematics, University of Leeds, Leeds, UK

Correspondence
Carmen Molina-París, Department of Applied Mathematics, School of Mathematics, University of Leeds, Leeds, UK.
Email: carmen@maths.leeds.ac.uk

Funding information
European Union FP7 Programme, Grant/Award Number: PIRSES-GA-2012-317893; European Union H2020 Programme, Grant/Award Number: 764698 MSCA-ITN-2017 (QuanTII ETN); Spanish Ministry of Economy, Grant/Award Numbers: FIS2016-78883-C2-2-P, PRX 16/00287

Interleukin-7 (IL7) plays a nonredundant role in T cell survival and homeostasis, which is illustrated in the severe T cell lymphopenia of IL7-deficient mice, or demonstrated in animals or humans that lack expression of either the IL7Rα or γ_c chain, the two subunits that constitute the functional IL7 receptor. Remarkably, IL7 is not expressed by T cells themselves, but produced in limited amounts by radio-resistant stromal cells. Thus, T cells need to constantly compete for IL7 to survive. How T cells maintain homeostasis and further maximize the size of the peripheral T cell pool in face of such competition are important questions that have fascinated both immunologists and mathematicians for a long time. Exceptionally, IL7 downregulates expression of its own receptor, so that IL7-signaled T cells do not consume extracellular IL7, and thus, the remaining extracellular IL7 can be shared among unsignaled T cells. Such an altruistic behavior of the IL7Rα chain is quite unique among members of the γ_c cytokine receptor family. However, the consequences of this altruistic signaling behavior at the molecular, single cell and population levels are less well understood and require further investigation. In this regard, mathematical modeling of how a limited resource can be shared, while maintaining the clonal diversity of the T cell pool, can help decipher the molecular or cellular mechanisms that regulate T cell homeostasis. Thus, the current review aims to provide a mathematical modeling perspective of IL7-dependent T cell homeostasis at the molecular, cellular and population levels, in the context of recent advances in our understanding of the IL7 biology.

This article is categorized under:

Models of Systems Properties and Processes > Organ, Tissue, and Physiological Models
Biological Mechanisms > Cell Signaling
Models of Systems Properties and Processes > Mechanistic Models
Analytical and Computational Methods > Computational Methods

KEYWORDS

cytokine, immunology, mathematical model, receptor, signalling

1 | INTRODUCTION

The IL7 receptor (IL7R) and its ligand, IL7, are essential and nonredundant drivers of T cell development and homeostasis (Park et al., 2010; Peschon et al., 1994; Raeber, Zurbuchen, Impellizzieri, & Boyman, 2018; Schluns, Kieper, Jameson, & Lefrançois, 2000; Tan et al., 2001; von Freeden-Jeffry et al., 1995). While T cells critically depend on IL7R signaling, IL7 itself is not expressed by T cells. Instead, IL7 is mostly expressed by stromal cells and non-T lineage lymphoid and myeloid cells (Kim, Hong, & Park, 2011), and the amount of IL7 production is considered to be developmentally set (Fry et al., 2001; Martin et al., 2017). Consequently, IL7 signaling at the single cell level is primarily controlled by IL7 receptor expression, and secondarily by IL7 availability in vivo. Thus, interrogating the molecular basis of IL7 receptor expression and regulation is important to understand the role of IL7 receptor signaling in T cell immunity.

The functional IL7 receptor is composed of the IL7-specific IL7Rα chain (CD127) and the common γ-chain (γ_c or CD132), which is shared with a series of other cytokines that include IL2, IL4, IL9, IL15, and IL21 (Waickman, Park, & Park, 2016). Since γ_c expression is presumed to be constitutive and also found in significant amounts on all T cells (Rochman, Spolski, & Leonard, 2009), much of the past and current studies of IL7 signaling have been focused on the regulatory mechanisms of the IL7Rα chain. Notably, the IL7 receptor harbors many unique features that complicate the assessment of IL7R signaling and its downstream effects. Among others, IL7 receptor signaling downregulates expression of its own receptor, so that IL7 signaling leads to suppression of further IL7R signaling (Park et al., 2004). Initiating such a negative regulatory feedback is quite unusual, because expression of most other members of the γ_c receptor family is upregulated by their cognate cytokine signals (Depper et al., 1985). Recent studies have shown that such unique behavior profoundly affects the kinetics and magnitude of IL7 receptor signaling, and that this regulatory mechanism is essential to maintain normal T cell development and homeostasis (Kimura et al., 2013; Munitic et al., 2004; Park et al., 2004). In fact, IL7-induced downregulation of IL7R prevents IL7 signaled T cells from further consumption of extracellular IL7, so that the limited amount of free IL7 can be shared among unsignaled T cells. Such altruistic behavior of the IL7R seems required to maximize the size and diversity of the peripheral T cell pool (Park et al., 2004). However, a greater understanding of the quantitative and qualitative immunological signaling effects, under continuous de-sensitization and resensitization of the IL7 receptor, requires stratification of the IL7 signaling components. We consider that assessing these issues at the molecular, single cell and population levels will benefit from mathematical modeling of this complex immune signaling pathway. Additionally, IL7Rα not only interacts with its ligand but also binds directly to γ_c proteins in the absence of IL7 (Hong et al., 2014; McElroy et al., 2012). As a result, IL7Rα and γ_c can exist as a preassociated, inactive receptor complex on the cell membrane, even prior to ligand engagement (Hong et al., 2014; McElroy et al., 2012). Receptor preassociation brings in a couple of new variables into the circuitry of IL7R signaling. Since the γ_c chain is a shared component of multiple cytokines, preassociation of γ_c with IL7Rα would sequester the γ_c chain from association with other cytokine receptors, such as IL15Rβ, and could interfere with their signaling capability in trans. Moreover, IL7Rα/γ_c preassociation would change the IL7 binding affinity of IL7Rα, so that free IL7Rα proteins would have lower IL7 affinities than IL7Rα complexed with γ_c. Because on the cell surface the number of IL7Rα molecules is thought to vastly outnumber that of γ_c proteins (Cotari, Voisinne, Dar, Karabacak, & Altan-Bonnet, 2013), under such a scenario, there would be two different species of IL7Rα chains, that is, free and γ_c-complexed, on the cell surface. Significantly, the free form would be signaling-incompetent and could act as an IL7 scavenger. On the other hand, the γ_c preassociated form would be signaling-competent, but outnumbered by unassociated IL7Rα proteins. How cellular exposure to IL7 would initiate signaling in cells that express a mixture of two distinct receptor species is an important question that could be addressed making use of the mathematical modeling methods presented in this review at the molecular, cellular and population scales (see Section 5.1).

Finally, enforced IL7 receptor expression does not promote, but paradoxically, inhibits both development and homeostasis of T cells (Kimura et al., 2013; Munitic et al., 2004). Whether this is due to excessive IL7 signaling on a per cell basis that would be detrimental for cell survival (Kimura et al., 2013), or because of excessive IL7 consumption on a population basis, that would further limit IL7 availability (Park et al., 2004), still needs to be clarified (Mazzucchelli & Durum, 2007). In addition, the IL7Rα chain has no intrinsic signaling capability and requires association with the tyrosine kinase JAK1, through its cytosolic tail, to trigger downstream signaling. But JAK1 proteins are unstable due to microRNA controlled post-transcriptional mechanisms, and this could potentially limit their availability for IL7Rα (Katz et al., 2014). Thus, in addition to the extracellular events that control IL7 signaling at the level of receptor and ligand association, the roles of intracellular components in the IL7R signaling machinery must also be considered (see Section 5.1).

Collectively, interrogating how these unique aspects of IL7 receptor signaling are interweaved in the control of T cell development and homeostasis is essential to unravel the basic mechanisms that regulate T cell-mediated immune responses at both the single cell and population levels. Computational and mathematical models of the dynamical interactions between these many elements (immune molecules and cells) have tremendously contributed to our understanding of cytokine receptor

signaling (Callard, George, & Stark, 1999; Cotari et al., 2013; Feinerman et al., 2010; Gonnord et al., 2018; Palmer et al., 2008; Reynolds, Coles, Lythe, & Molina-París, 2013), and quantitative approaches and tools are also essential and required to dissect the contribution of individual nodes in the IL7 signaling pathway.

In this review, we highlight the current state of our knowledge of the basic IL7 receptor biology and focus on the role IL7 and IL7R have on mature $CD8^+$ T cells as drivers of survival and homeostasis. Furthermore, we document recent advances in the mathematical and computational modeling of IL7 receptor signaling and its application in furthering our understanding of the dynamics of immune receptor signaling at the molecular (see Section 5.1), cellular (see Section 5.2) and population levels (see Section 5.3).

2 | IL7 RECEPTOR EXPRESSION AND FUNCTION IN T CELL DEVELOPMENT AND HOMEOSTASIS

The signaling-competent IL7 receptor is a hetero-dimeric protein complex, composed of the specific IL7Rα chain and the γ_c receptor. In contrast to γ_c expression, IL7Rα expression is dynamically regulated during T cell development and differentiation, so that IL7Rα expression is the primary determinant of IL7 responsiveness (Mazzucchelli & Durum, 2007). During thymocyte development, IL7Rα is highly expressed on the most immature $CD4^-$, $CD8^-$ double-negative (DN) cells, but then terminated upon differentiation into $CD4^+$, $CD8^+$ double-positive (DP) cells (McCaughtry et al., 2012; Park et al., 2016; Yu et al., 2006). IL7Rα signaling is required in immature DN cells to provide critical prosurvival and proliferative cues (Kim, Lee, Sayers, Muegge, & Durum, 1998; Peschon et al., 1994). However, continued IL7Rα expression on DP thymocytes is detrimental to T cell development, since it would interfere with selection of a T cell receptor (TCR)-dependent immunocompetent repertoire (Munitic et al., 2004; Yu, Erman, Park, Feigenbaum, & Singer, 2004). The molecular mechanism that terminates IL7Rα protein expression and transcription on DP thymocytes is not known (Ligons et al., 2012). Interestingly, this feature is not evolutionary conserved, because DP thymocytes in humans express robust amounts of IL7Rα proteins (Marino et al., 2010). Nonetheless, immature DP thymocytes in humans show dramatic downregulation of γ_c protein expression, which renders these cells IL7 unresponsive (Marino et al., 2010). Thus, suppression of IL7R signaling in DP thymocytes is a common characteristic in both mice and humans, but that is achieved through different means.

TCR-induced positive selection results in reexpression of IL7Rα on both $CD4^+$ and $CD8^+$ lineage T cells (Yu et al., 2006). Concomitant to IL7Rα upregulation, $CD8^+$ lineage committed thymocytes become IL7-responsive. $CD4^+$ lineage committed cells, on the other hand, remain IL7 unresponsive despite expressing large amounts of IL7Rα. In fact, it is the selective de-sensitization of cytokine receptors in $CD4^+$ lineage cells that determines CD4/CD8 lineage choice in the thymus and imposes $CD4^+$ lineage choice (Singer, Adoro, & Park, 2008). Mechanistically, it was recently demonstrated that expression of the $CD4^+$ lineage-specific transcription factor ThPOK induces expression of Suppressor Of Cytokine Signaling (SOCS) genes, which in turn suppresses IL7R signaling to prevent upregulation of the CD8-specifying transcription factor Runx3 (Luckey et al., 2014). Thus, surface IL7Rα expression does not necessarily guarantee productive IL7R signaling. Along this line, cytokine receptor de-sensitization is another mechanism that needs to be considered to understand IL7 receptor signaling.

Multiple mechanisms have been proposed to induce de-sensitization of IL7Rα signaling. Persistent TCR signaling that leads to destabilization of IL7Rα-associated JAK1 expression, or upregulation of SOCS1 expression to inhibit JAK kinase activity, and proteolytic cleavage of the γ_c chain cytosolic tail by the cysteine protease, calpain, are some of the proposed, and not necessarily mutually exclusive, mechanisms (Chong et al., 2003; Katz et al., 2014; Noguchi et al., 1997). During thymocyte differentiation, regaining IL7 responsiveness is critical for $CD8^+$ single positive (SP) thymocyte generation because impaired IL7 signaling, either by enforced expression by SOCS1 or by conditional deletion of IL7Rα in preselection thymocytes, resulted in profoundly impaired generation of $CD8^+$ lineage cells (Luckey et al., 2014; McCaughtry et al., 2012; Park et al., 2010). The prerequisite for IL7 signaling in $CD8^+$ cells is mostly due to a STAT5 requirement, which upregulates expression of Runx3 and induces expression of a series of prosurvival molecules, including Bcl-2 and Mcl-1 (Akashi, Kondo, von Freeden-Jeffry, Murray, & Weissman, 1997; Opferman et al., 2003). However, IL7 also activates other downstream signaling pathways, such as PI-3 K and NFATc1, which contribute to cell survival by upregulation of antiapoptotic molecules and trophic factors, including expression of the glucose transporter-1 (Rathmell, Farkash, Gao, & Thompson, 2001; Wofford, Wieman, Jacobs, Zhao, & Rathmell, 2008; Yu, Erman, Bhandoola, Sharrow, & Singer, 2003).

Upon their generation in the thymus, T cells move out to peripheral tissues but they remain addicted to IL7 throughout their life. Thus, maintaining high levels of IL7Rα expression on mature T cells is critical for T cell survival. However, the regulatory mechanism of IL7Rα transcription is quite distinct between thymocytes and peripheral T cells. Previously, an evolutionary conserved enhancer element, CNS1, had been identified that sits 3.6 kb upstream of the IL7Rα promoter (Lee, Shibata, Ogawa, Maki, & Ikuta, 2005), and which was found to be controlled by multiple factors, including FoxO1 and Foxp1, as well as glucocorticoids (Feng et al., 2011; Kerdiles et al., 2009; Lee et al., 2005). Remarkably, deletion of CNS1

resulted in dramatic loss of IL7Rα expression and significantly reduced T cell numbers in the periphery, but did not affect IL7Rα expression on thymocytes or decreased thymic cellularity (Abe et al., 2015). These results suggested the use of distinct molecular mechanisms to control IL7Rα chain expression on immature and mature T cells, and also echo previous observations of different IL7Rα regulatory mechanisms between $CD4^+$ and $CD8^+$ T cells (Ligons et al., 2012; Park et al., 2004) and also B and T lineage cells (DeKoter, Lee, & Singh, 2002; Xue et al., 2004). Thus, IL7Rα expression is regulated in a highly specific manner, depending on the developmental stage and possibly also on the activation status of T cells.

3 | REGULATION OF IL7 RECEPTOR EXPRESSION

A distinguishing feature of IL7Rα from other cytokine receptors of the γ_c family is the downregulation of its own expression by cognate cytokine signaling (Park et al., 2004). In fact, not only IL7, but other γ_c cytokines also transcriptionally suppress IL7Rα (Park et al., 2004; Xue et al., 2004). IL7-induced downregulation of IL7Rα expression is further accelerated by rapid endocytosis and degradation of IL7-associated IL7Rα proteins, so that IL7 induces a negative regulatory feedback loop for IL7 receptor signaling (Faller, Ghazawi, Cavar, & MacPherson, 2016; Henriques, Rino, Nibbs, Graham, & Barata, 2010). Considering the critical role of IL7 in T cell survival and the limited availability of IL7 in vivo, it seems paradoxical that IL7 signaling would terminate further IL7 signaling.

Two distinct but not mutually exclusive hypotheses have been put forward to explain the self-limiting nature of IL7 receptor signaling on T cells. The first model proposes that T cells constrain IL7 signaling and consumption to maximize the use of limited extracellular IL7 and to maintain clonal diversity of the mature peripheral T cell pool (Park et al., 2004). By preventing excess consumption of IL7 and clonal outgrowth of T cells that have better access to IL7, on a population basis, IL7-induced IL7Rα downregulation would maximize the size of the T cell pool, while maintaining a high degree of TCR clonal diversity. Thus, IL7Rα downregulation would be beneficial for a population, but not for individual T cells per se. Contrary to this idea, the second model proposes that sustained IL7 signaling would be detrimental for individual T cells, and that termination of prolonged IL7 signaling is necessary for survival. In fact, in vivo transfer experiments and in vitro proliferation assays with IL7Rα transgenic T cells demonstrated that the inability to downregulate IL7Rα expression resulted in cytokine-induced cell death of T cells (Kimura et al., 2013). Specifically, continuous IL7R signaling in $CD8^+$ T cells resulted in their uncontrolled proliferation and rapid differentiation into effector cytolytic T cells that produced large amounts of interferons and induced cell death. In agreement, IL7Rα-transgenic mice also contain a significantly reduced size of T cell pool in the periphery (Kimura et al., 2013; Park et al., 2004).

The molecular mechanisms that lead to suppression of IL7Rα expression have been assessed, and at least for $CD8^+$ T cells, it was found to be dependent on the zinc finger transcription factor Gfi1 (Park et al., 2004). $CD8^+$ T cells in Gfi1-deficient mice expressed high levels of IL7Rα, while $CD8^+$ T cells in Gfi1-transgenic mice showed reduced IL7Rα transcription and expression (Ligons et al., 2012; Opferman et al., 2003). The cellular factors that control IL7Rα suppression in $CD4^+$ T cells are less well known. But reportedly, the forkhead box family transcription factor Foxp3 downregulates IL7Rα expression on $Foxp3^+$ T regulatory $CD4^+$ T cells (Liu et al., 2006), and Foxp1 can suppress IL7Rα by antagonizing Foxo1 (Feng et al., 2011). The precise transcriptional pathway that controls IL7Rα downstream of IL7 and other cytokine signals remains to be mapped.

4 | IL7 RECEPTOR SIGNALING

Both IL7Rα and γ_c chains lack intrinsic kinase activities. Rather, they require activation of the tyrosine kinases JAK1 and JAK3, which are constitutively associated with the cytosolic tails of IL7Rα and γ_c, respectively, to transduce IL7 signaling (Waickman et al., 2016). Upon ligand-induced IL7Rα/γ_c hetero-dimerization, JAK1 and JAK3 trans-activate each other, and subsequently phosphorylate the intracellular tail of IL7Rα. There are three conserved tyrosine residues in the IL7Rα cytosolic domain, but tyrosine 449 is the major substrate of IL7Rα phosphorylation (Jiang et al., 2004). Phosphorylation of IL7Rα Tyr449 leads to the creation of STAT5 and PI-3-kinase binding sites, resulting in the recruitment and subsequent phosphorylation and activation of these factors (Jiang et al., 2004; Venkitaraman & Cowling, 1994).

Due to their distinct ligand binding affinities and association with different JAK molecules, the individual contribution of each IL7R subunit to IL7 signaling also differs. The γ_c chain contributes to IL7 receptor signaling through two major activities. First, it serves to bring JAK3 into the receptor signaling complex, which trans-activates IL7Rα-bound JAK1 (Waickman et al., 2016). Second, γ_c dramatically increases the affinity of the IL7 receptor complex for IL7. In the absence of γ_c, IL7Rα binds IL7 with a low affinity (Noguchi et al., 1993) ($K_d = 2.4 \times 10^{-10}$ M). However, inclusion of γ_c significantly increases the affinity for IL7 ($K_d = 4 \times 10^{-11}$ M), which results in the preferential capture of IL7 by signaling-competent IL7 receptors

compared to signaling-incompetent γ_c-free IL7Rα chain proteins. Whether the high affinity IL7Rα/γ_c complex is only formed upon ligand binding, or whether such high affinity IL7 receptor could be already assembled and expressed on the cell surface is currently a much-debated issue in cytokine biology.

The conventional view posits that the IL7Rα/γ_c complex is formed by stepwise assembly that is triggered by IL7 binding to the IL7Rα chain (Shimizu, Kondo, Sabe, Ishida, & Honjo, 1986). In this model, the IL7Rα and γ_c proteins are diffusely distributed in the plasma membrane prior to ligand engagement. Upon IL7 stimulation, IL7Rα binds IL7 with low affinity and undergoes a conformational change that attracts the γ_c chain, which in turn stabilizes IL7 binding, to initiate IL7R signaling. The formation of a hetero-trimeric complex of IL7/IL7Rα/γ_c brings the intracellular tails of IL7Rα and γ_c into proximity, which juxtapositions and activates JAK1 and JAK3 to initiate downstream signaling.

In an alternative view, it has been proposed that IL7Rα and γ_c can bind even in the absence of IL7, so that γ_c proteins are already sequestered and associated with IL7Rα (McElroy et al., 2012; Walsh, 2012). In fact, crystallographic studies of the IL7Rα/γ_c receptor complex postulated that IL7Rα and γ_c proteins exist as preformed, inactive receptor complexes prior to ligand engagement (McElroy et al., 2012). In this model, ligand-free IL7Rα and γ_c associate in a "head-to-head" configuration that pushes away the trans-membrane domains and intracellular tails of IL7Rα and γ_c, and thus, prevents spontaneous ligand-independent activation of JAK1 and JAK3. Upon IL7 binding, however, the preassociated IL7Rα/γ_c complex undergoes a conformational change that erects the receptor complex and brings the intracellular tails of IL7Rα/γ_c into close proximity and initiates downstream signaling (McElroy et al., 2012).

Currently, it is not clear which one of these strategies is employed by T cells for IL7 receptor signaling. Direct binding of IL7Rα to γ_c proteins on the cell surface could be potentially visualized and quantified by FRET (Fluorescence Resonance Energy Transfer) microscopy. Alternatively, methods such as PLA (Proximity Ligation Assays) could be also employed to demonstrate preassembly of γ_c with IL7Rα (Fredriksson et al., 2002). At least in human $CD4^+$ T cells, IL7Rα could be coimmunoprecipitated with γ_c in the absence of IL7, which is in support of the IL7Rα/γ_c preassociation model (Rose et al., 2010). Whether a stepwise assembly model, where initially all surface IL7 receptors have the same affinity to IL7, or the preassembly model, where two classes of IL7 receptor exist and the functionally competent IL7Rα/γ_c complexes would out-compete low affinity IL7Rα receptors, would be more biologically meaningful is not clear. However, we consider this question precisely an area where mathematical modeling can be employed to compare and test these different hypotheses (or mechanisms) together with empirical data. Thus, in the following section, we illustrate the power of a quantitative mathematical approach by modeling the molecular regulation of IL7R signaling under the scenario where two homeostatic γ_c family cytokines, namely IL7 and IL15, compete for the γ_c chain (see Section 5.1). At the single cell level, we quantify the effect of the altruistic hypothesis on the number of IL7R molecules expressed on the membrane of T cells (see Section 5.2). Finally, at the population scale, we model the heterogeneity of T cell responses to IL7 stimulation observed in Palmer, Mahajan, Chen, Irvine, and Lauffenburger (2011), where IL7 availability and the existence of survival and proliferation thresholds can influence the population dynamics of IL7 dependent T cells (see Section 5.3).

5 | MATHEMATICAL MODELS AT THE MOLECULAR, CELLULAR AND POPULATION LEVELS

5.1 | Mathematical model at the molecular level

At the molecular level, we are interested in understanding the role of shared components in immune signaling (Palmer et al., 2008). In the case of IL7R signaling, a first shared component is the γ_c chain, which is part of the hetero-dimeric receptors IL7R and IL15R (see Figure 1). The γ_c chain is also part of the hetero-trimeric receptor IL2R (Waldmann, 2015). In this review, we have chosen to consider the IL15R as a shared component of the IL7 signaling pathway, since there already exists a significant mathematical effort to describe the IL2R one (Busse et al., 2010; de la Higuera, López-García, Lythe, & Molina-París, 2017; Fallon & Lauffenburger, 2000; Feinerman et al., 2010; Gonnord et al., 2018).

Let us now describe the shared elements of IL7R and IL15R. In principle, the γ_c receptor subunit can bind to either the IL7Rα or IL15Rβ chains, forming two different hetero-dimeric receptors for IL7 and IL15, respectively.

Although γ_c contributes with the same stoichiometry to each hetero-dimeric receptor (IL7R and IL15R), only when the trimeric complex IL7/IL7Rα/γ_c is internalized, downstream signaling is initiated, as discussed in Section 4 (in Section 5.2, we discuss receptor internalization in greater detail from a mathematical modeling perspective). Thus, the presence of IL15 can, indirectly, sequester γ_c and, reduce IL7R signaling. Note that we denote by IL7R, the hetero-dimeric receptor composed of one molecular unit of γ_c and one molecular unit of IL7Rα, and by IL15R, the hetero-dimeric receptor composed of one molecular unit of γ_c and one molecular unit of IL15Rβ. In this context, it is important to refer to the recent work by the groups of K. C. García and I. Moraga, who have been able to engineer *synthekines*, namely, engineered ligands, that produce

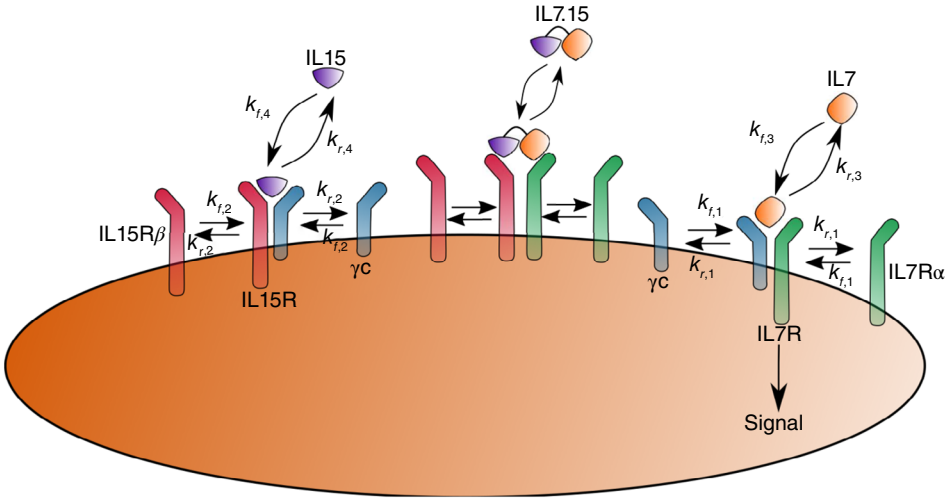

FIGURE 1 An example of shared molecular components in immune signaling: competition for the γ_c chain by the IL7Rα and IL15Rβ chains (adapted from Palmer et al. (2008))

"unnatural" receptor pairings, yet activate distinct signaling programs (Moraga et al., 2017). In Figure 1, we show one such potential synthekine, formed by IL7 and IL15, and denoted IL7.15. In this paper, we do not consider ligand-induced receptor dimerization (for simplicity, and assume both receptor chains have already formed the hetero-dimeric receptor before ligand binding), although, it may be relevant for some combtinations of γ_c and cytokine receptors (Cotari et al., 2013).

5.1.1 | Mathematical model

Following Palmer et al. (2008), we model the dynamics of free IL7 and IL15 cytokines (or ligands), the receptor subunits γ_c, IL7Rα and IL15Rβ and the (complex) hetero-dimeric receptors IL7R and IL15R, either bound or unbound to their respective ligands. We note that in this review, we do not consider the presence of synthetic ligand IL7.15. We consider the molecular reactions described in Figure 1, which include the association and dissociation of different receptor chains, as well as the association and dissociation of ligand (IL7 or IL15) to the hetero-dimeric receptors IL7R and IL15R, respectively. We are interested in understanding how the concentrations of these molecular species evolve in time. This is described in Palmer et al. (2008) by the following system of ordinary differential equations (ODEs)

$$
\begin{aligned}
\frac{d[\mathrm{IL7R}\alpha]}{dt} &= -k_{f,1}[\mathrm{IL7R}\alpha][\gamma_c] + k_{r,1}[\mathrm{IL7R}]_u,\\
\frac{d[\mathrm{IL15R}\beta]}{dt} &= -k_{f,2}[\mathrm{IL15R}\beta][\gamma_c] + k_{r,2}[\mathrm{IL15R}]_u,\\
\frac{d[\gamma_c]}{dt} &= -k_{f,1}[\mathrm{IL7R}\alpha][\gamma_c] + k_{r,1}[\mathrm{IL7R}]_u - k_{f,2}[\mathrm{IL15R}\beta][\gamma_c] + k_{r,2}[\mathrm{IL15R}]_u,\\
\frac{d[\mathrm{IL7R}]_u}{dt} &= k_{f,1}[\mathrm{IL7R}\alpha][\gamma_c] - k_{r,1}[\mathrm{IL7R}]_u - k_{f,3}[\mathrm{IL7}][\mathrm{IL7R}]_u + k_{r,3}[\mathrm{IL7R}]_b,\\
\frac{d[\mathrm{IL15R}]_u}{dt} &= k_{f,2}[\mathrm{IL15R}\beta][\gamma_c] - k_{r,2}[\mathrm{IL15R}]_u - k_{f,4}[\mathrm{IL15}][\mathrm{IL15R}]_u + k_{r,4}[\mathrm{IL15R}]_b,\\
\frac{d[\mathrm{IL7R}]_b}{dt} &= k_{f,3}[\mathrm{IL7}][\mathrm{IL7R}]_u - k_{r,3}[\mathrm{IL7R}]_b,\\
\frac{d[\mathrm{IL15R}]_b}{dt} &= k_{f,4}[\mathrm{IL15}][\mathrm{IL15R}]_u - k_{r,4}[\mathrm{IL15R}]_b.\\
\frac{d[\mathrm{IL7}]}{dt} &= -k_{f,3}[\mathrm{IL7}][\mathrm{IL7R}]_u + k_{r,3}[\mathrm{IL7R}]_b,\\
\frac{d[\mathrm{IL15}]}{dt} &= -k_{f,4}[\mathrm{IL15}][\mathrm{IL15R}]_u + k_{r,4}[\mathrm{IL15R}]_b.
\end{aligned}
$$

These equations can be solved for different initial conditions of ligand concentration of IL7 and IL15, as well as different number of receptor chains (γ_c, IL7Rα and IL15Rβ) (Palmer et al., 2008) (see Table 1). The table below provides the values of the association and dissociation rates considered in the model (Palmer et al., 2008), and the different initial conditions that have been considered.

TABLE 1 Summary of parameters used in the molecular model of Section 5.1. Parameter values have been taken from Palmer et al. (2011)

Parameter	Value	Units
ρ (cell density)	10^5	cells/μL
[IL7]($t = 0$)	10^{-1}–10^3	nM
[IL15]($t = 0$)	10^{-1}–10^3	nM
[IL7Rα]($t = 0$)	10^3	cell^{-1}
[IL15Rβ]($t = 0$)	10^3	cell^{-1}
[γ_c]($t = 0$)	10–10^5	cell^{-1}
$k_{f,\,1}$	1	nM^{-1} min^{-1}
$k_{r,\,1}$	0.1	min^{-1}
$k_{f,\,2}$	1	nM^{-1} min^{-1}
$k_{r,\,2}$	0.1	min^{-1}
$k_{f,\,3}$	1	nM^{-1} min^{-1}
$k_{r,\,3}$	0.1	min^{-1}
$k_{f,\,4}$	0.1	nM^{-1} min^{-1}
$k_{r,\,4}$	0.1	min^{-1}

In Figure 2 (left plot), we show the effect of the initial concentration of IL7, [IL7]($t = 0$), on the steady state value of the relative fraction of bound IL7 receptors, $[\text{IL7R}]_b$, defined as follows:

$$f_7 = \lim_{t \to +\infty} \frac{[\text{IL7R}]_b(t)}{[\text{IL7R}]_b(t) + [\text{IL15R}]_b(t)}. \tag{1}$$

Figure 2 (middle plot) shows the effect of the initial concentration of IL15, [IL15]($t = 0$), on f_7. We note that f_7 decreases as the initial concentration of [IL15]($t = 0$) increases, as expected. The green curve in Figure 2 can be reproduced using the language BioNetGen (Blinov, Faeder, Goldstein, & Hlavacek, 2004; Faeder, Blinov, & Hlavacek, 2009; Sekar & Faeder, 2017) and the listing in Appendix A. Minimal modifications of the code will allow the reader to obtain the rest of the plots in Figure 2. Finally, the right plot, shows for an initial concentration of [IL15] = 9.5 nM (the IL15 concentration that yields $[\text{IL7R}]_b = [\text{IL15R}]_b$ at steady state), the effect of the initial value of γ_c chain expression on the steady state values of $[\text{IL7R}]_b$ and $[\text{IL15R}]_b$.

5.2 | Mathematical model at the cellular level

The role of the IL7 receptor in T cell development, homeostasis and differentiation has been widely studied and recognized (Mazzucchelli & Durum, 2007; Takada & Jameson, 2009). IL7Rα cell surface expression on T cells is downregulated once a T cell has received enough survival signals mediated by IL7R (Mazzucchelli & Durum, 2007; Park et al., 2004). To model this

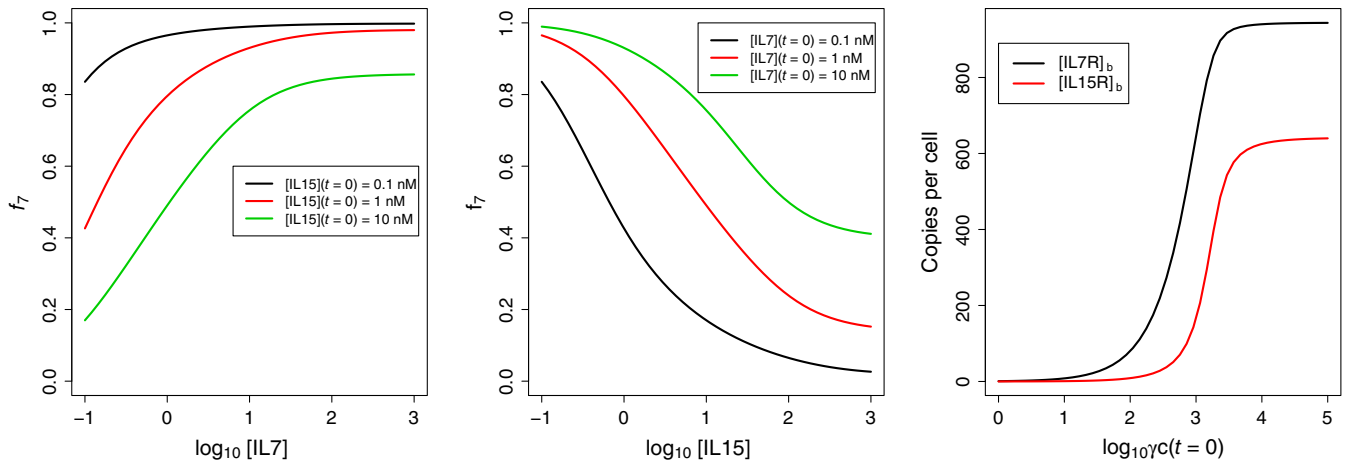

FIGURE 2 Left plot: fraction of bound $[\text{IL7R}]_b$, f_7, as defined by Equation (1), for different values of the initial concentration of [IL7]($t = 0$). Different colors correspond to different values of the initial concentration of [IL15]($t = 0$), as shown in the legend. Middle plot: fraction of bound $[\text{IL7R}]_b$, f_7, as in the left panel, but as a function of the initial concentration of [IL15]($t = 0$). Right plot: steady state values for the bound complexes, $[\text{IL7R}]_b$ and $[\text{IL15R}]_b$, as a function of the initial γ_c chain expression, $\gamma_c(t = 0)$. The parameters have been taken from Palmer et al. (2011) and have been summarized in Table 1

so-called *altruistic* downregulation of membrane IL7R, we note that, upon IL7 stimulation, there is rapid IL7Rα internalization (mediated by endocytosis), that is accompanied with a reduced rate of receptor recycling and increased receptor degradation (Henriques et al., 2010). Thus, we first formulate a simple mathematical model (for further details, see Reynolds et al. (2013)), which describes the dynamics of the number of *ligand molecules* (IL7, in this case), $m_1(t)$, and per cell free-receptor (IL7R), $m_2(t)$, binding/unbinding to form a receptor-ligand bound complex, $m_3(t)$, internalization, degradation and recycling. We also assume that cell signaling is elicited (and encoded in the dynamics of the variable, $m_4(t)$, which represents a potential unidentified transcription factor), after bound receptors are internalized, as reported in Henriques et al. (2010). Finally, the altruistic effect (Park et al., 2004) is included as a signal-dependent synthesis rate (Reynolds et al., 2013). We note that recent experimental evidence suggests that IL7 availability is regulated by innate lymphoid cells (ILCs), which act as a "cytokine sink" by competing for and consuming IL7 and thus, restricting T cell homeostasis in lymphoid organs. In fact, ILCs seem to outcompete T cells for IL7 by resisting IL7-mediated IL7R downregulation (Friedrich & Gasteiger, 2017), which would support the idea that ILCs do not behave in an altruistic manner.

5.2.1 | A simple model of altruistic IL7Rα dynamics

Mathematically, we describe the time evolution of the IL7 and IL7R in a cellular model (see Reynolds et al. (2013)) making use of a system of ordinary differential equations (ODEs), as follows

$$\frac{dm_1}{dt} = \phi + N_c(k_{\text{off}}\ m_3 - k_{\text{on}}\ m_1\ m_2), \tag{2}$$

$$\frac{dm_2}{dt} = -k_{\text{on}}\ m_1\ m_2 + k_{\text{off}}\ m_3 - \sigma_u\ m_2 + \frac{\kappa_s}{\kappa_s + m_4}\xi, \tag{3}$$

$$\frac{dm_3}{dt} = k_{\text{on}}\ m_1\ m_2 - k_{\text{off}}\ m_3 - \sigma_b\ m_3, \tag{4}$$

$$\frac{dm_4}{dt} = \psi\ m_3 - \chi\ m_4, \tag{5}$$

where ϕ is the rate at which free IL7 is replenished in the extracellular volume (source term), N_c is the total number of cells (in the experiment), k_{on} and k_{off} are, respectively, the binding and unbinding rates of IL7 and IL7R, σ_u and σ_b are the internalization rates of the unbound and bound receptors (following Henriques et al. (2010) and Reynolds et al. (2013), we assume $\sigma_b > \sigma_u$), ξ is the rate at which IL7R receptor is synthesized and transported to the cell membrane, κ_s is the carrying capacity of m_4, which accounts for the altruistic effect. Note that in the limit $\kappa_s \to 0^+$ we have perfect altruism (as IL7R synthesis after receptor internalization is fully inhibited). On the other hand, in the limit $\kappa_s \to +\infty$, the rate of synthesis is independent of signaling, and thus, there is no altruistic feedback (as might be the case for ILCs (Friedrich & Gasteiger, 2017)),[1] ψ is the rate at which internalized bound receptors elicit a signal (encoded by the potential unidentified transcription factor, m_4), and χ is the characteristic degradation rate of the signal (encoded by the potential unidentified transcription factor, m_4).

5.2.2 | Steady state analysis of the cellular model

In steady state, the system of equations, Equations (2) to (5), can be solved analytically. The solution is given by

$$m_1^{ss} = \frac{\phi(k_{\text{off}} + \sigma_b)\sigma_u(\kappa_s N_c \sigma_b \chi + \phi\psi)}{k_{\text{on}}\sigma_b\left[\kappa_s N_c \sigma_b \chi(N_c\xi - \phi) - \phi^2\psi\right]}\ , \tag{6}$$

$$m_2^{ss} = \frac{1}{N_c\sigma_u}\left[\frac{\kappa_s N_c^2 \sigma_b \xi \chi}{\kappa_s N_c \sigma_b \chi + \phi\psi} - \phi\right]\ , \tag{7}$$

$$m_3^{ss} = \frac{\phi}{N_c\sigma_b}\ , \tag{8}$$

$$m_4^{ss} = \frac{\phi\psi}{N_c\sigma_b\chi}\ . \tag{9}$$

These steady state solutions are positive as long as

$$\phi < \phi_{\text{threshold}} \equiv \frac{\sqrt{\kappa_s N_c^2 \sigma_b \chi(\kappa_s \sigma_b \chi + 4\psi\xi)} - \kappa_s N_c \sigma_b \chi}{2\psi}\ .$$

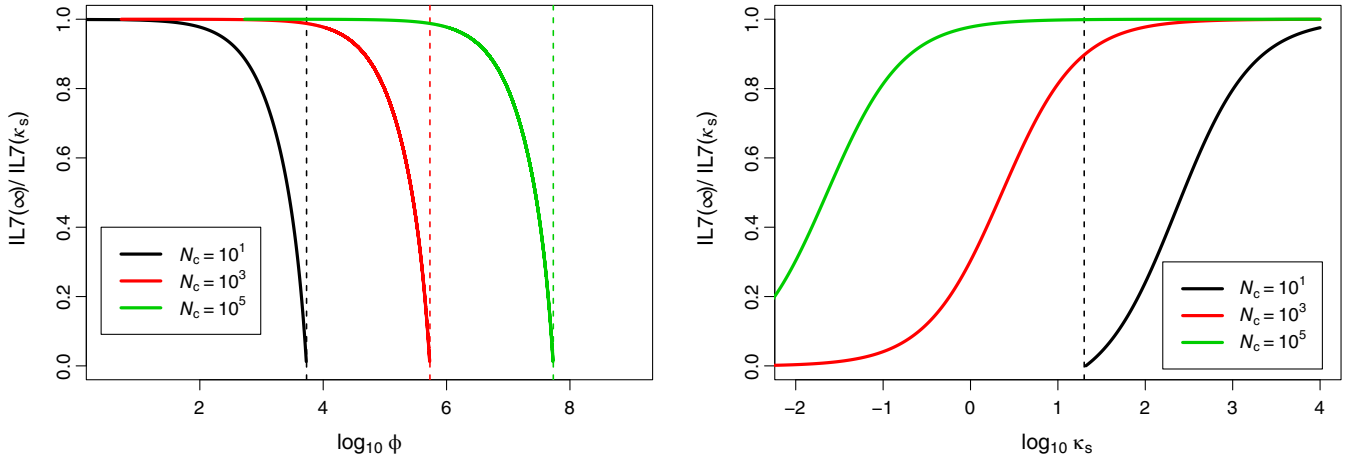

FIGURE 3 Effect of signaling altruism on the amount of available extracellular (free) IL7. Left plot: effect of ϕ for $\kappa_s = 10^3$ on $\frac{m_1^{ss}(\kappa_s \to +\infty)}{m_1^{ss}(\kappa_s)}$ for different values of N_c. Right plot: effect of κ_s for $\phi = \phi_{\text{threshold}}/2$ on $\frac{m_1^{ss}(\kappa_s \to +\infty)}{m_1^{ss}(\kappa_s)}$ for different values of N_c. Model parameters are summarized in Table 2. Different colors correspond to different values of the number of cells, N_c, in the experiment

Note that the limit, $\kappa_s \to +\infty$, in the steady state solutions given above, corresponds to a receptor-ligand system in which no cellular altruistic behavior is present. Let us now assess the effect of altruism in the different observables of the cellular system. For instance, in Figure 3 we plot $\frac{m_1^{ss}(\kappa_s \to +\infty)}{m_1^{ss}(\kappa_s)}$, the steady state ratio of free (available for other cells) IL7 in the nonaltruistic ($\kappa_s \to +\infty$) and altruistic ($\kappa_s \neq 0$) cases, for different values of ϕ (left plot) and for different values of κ_s (right plot). Similarly, in Figure 4 we plot $\frac{m_2^{ss}(\kappa_s)}{m_2^{ss}(\kappa_s \to +\infty)}$, the steady state ratio of free receptors (IL7R) in the nonaltruistic ($\kappa_s \to +\infty$) and altruistic ($\kappa_s \neq 0$) cases, for different values of ϕ (left plot) and for different values of κ_s (right plot). Note the symmetry between Figures 3 and 4. This is due to the fact that in steady state, one can show

$$\lim_{t \to +\infty} [\text{IL7}](t)[\text{IL7R}]_u(t) = \frac{\phi(k_{\text{off}} + \sigma_b)}{k_{\text{on}} N_c \sigma_b}, \tag{10}$$

which does not depend on the value of κ_s, the parameter which encodes the level of altruism in the IL7 signaling system.

5.3 | Mathematical model at the population level

Naive CD8$^+$ T cells require signaling-mediated by the cytokine interleukin-7 (IL7) for survival and proliferation (Takada & Jameson, 2009). As discussed in Palmer et al. (2011), CD8$^+$ T cells have distinct thresholds for survival and proliferation; that

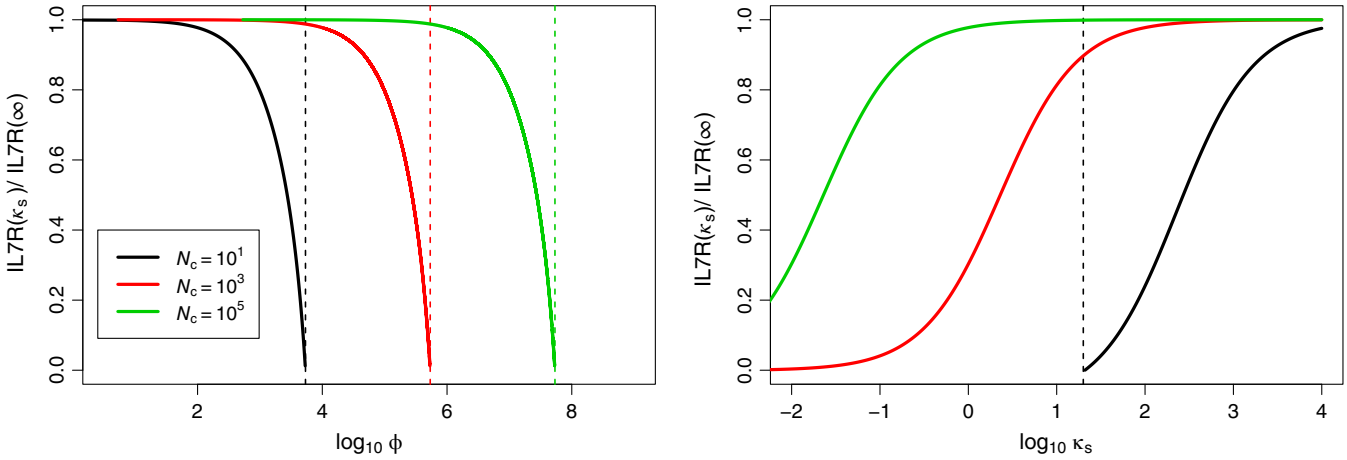

FIGURE 4 Effect of altruism on the amount of free IL7R. Left plot: effect of ϕ for $\kappa_s = 10^3$ on $\frac{m_2^{ss}(\kappa_s)}{m_2^{ss}(\kappa_s \to +\infty)}$ for different values of N_c. Right plot: effect of κ_s for $\phi = \phi_{\text{threshold}}/2$ on $\frac{m_2^{ss}(\kappa_s)}{m_2^{ss}(\kappa_s \to +\infty)}$ for different values of N_c. Model parameters are summarized in Table 2. Different colors correspond to different values of the number of cells, N_c, in the experiment

TABLE 2 Parameters of the cellular model taken from Reynolds et al. (2013) and Henriques et al. (2010)

Parameter	Value	Units
ϕ	10^1–10^8	receptor hour^{-1}
ξ	1.2×10^3	receptor hour^{-1}
κ_s	10^3	signal
σ_U	0.14	hour^{-1}
σ_B	1.4	hour^{-1}
$k_{\text{off}}/k_{\text{on}}$	1.7	ng ml^{-1}
ψ	0.61	signal receptor^{-1} hour^{-1}
χ	0.19	hour^{-1}

is, a stronger IL7R-mediated signal is required for proliferation as compared to the strength of signal required for cellular survival. Recent experiments also support the idea that higher CD5 expression correlates with higher IL7R expression in CD8$^+$ T cells, and indeed CD5$^{\text{hi}}$ T cells were found to have more robust responses to IL7 than CD5$^{\text{lo}}$ T cells (Palmer et al., 2011). On the other hand CD5$^{\text{lo}}$ T cells were found to have prolonged survival when compared to CD5$^{\text{hi}}$ T cells in an IL7 independent environment (Palmer et al., 2011).

In this section, we develop a mathematical model at the population level of immune IL7R-mediated signaling that considers the heterogeneity of the expression levels observed for CD5 and IL7R. We introduce, thus, four different CD8$^+$ T cell populations (see Figure 5), characterized by their relative expression of these two proteins. We also assume the total pool of CD8$^+$ T cells exists within a well-mixed system, such that there exists a global concentration of IL7. Thus, we neglect any spatial heterogeneities. T cells may receive signals for survival or proliferation depending on the amount of available extracellular IL7 and their relative IL7R surface expression. Since we are considering the dynamics of T cells at the population scale, we assume the effects of localized IL7 production and consumption at the single cell scale, are effectively "averaged out" allowing the modeling effort to give a reasonable description of the population dynamics (Palmer et al., 2008; Reynolds et al., 2013).

The physical size of the IL7 protein is much smaller than the size of a T cell and typically there are many more of these molecules than T cells in the experimental system. Our measurement of IL7 will, therefore, not be based on the number of IL7 molecules, but rather the concentration of IL7 in the extracellular medium. Therefore, we use a deterministic characterization for the IL7 concentration, instead of a stochastic description, which shall be introduced to describe the number of T cells in the system. We assume the rate of production of IL7 is independent of the number of T cells (Fry & Mackall, 2002), and for the purposes of this model, we will assume the rate of IL7 production to be constant. We also assume the rate of consumption

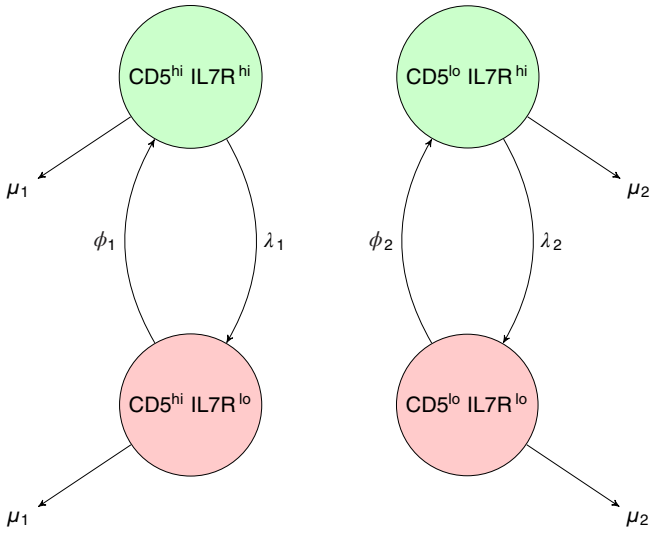

FIGURE 5 Immune signaling at the population level: possible transitions between the four subsets of the peripheral CD8$^+$ T cell pool. We impose $\mu_1 > \mu_2$; that is, CD5$^{\text{lo}}$ T cells have prolonged survival in a cytokine independent environment. In the mathematical model the parameter λ corresponds to the per cell division rate. λ_1 is the per cell division rate for CD5$^{\text{hi}}$ CD8$^+$ T cells and λ_2 is the per cell division rate for CD5$^{\text{lo}}$ CD8$^+$ T cells, with $\lambda_1 > \lambda_2$ (Palmer et al., 2011). We assume that after a division event, there is a significant drop in the level of IL7R expressed on the surface of a cell, since daughter cells inherit, on average, half of the IL7 receptors expressed by their mother cell. Finally, ϕ corresponds to the basal upregulation rate of IL7R expression and is assumed to be independent of the extracellular IL7 concentration. ϕ_1 is the per cell IL7R upregulation rate for CD5$^{\text{hi}}$ CD8$^+$ T cells and ϕ_2 is the per cell IL7R upregulation for CD5$^{\text{lo}}$ CD8$^+$ T cells

of IL7 is proportional to the product of the concentration of IL7 and the number of T cells expressing IL7R, due to the internalization of ligand-receptor bound complexes (see Section 5.1). The constants of proportionality are greater/lower for $IL7R^{hi}$/$IL7R^{lo}$ T cells, respectively. We further assume that the four different T cell populations have a basal IL7-independent death rate. This death rate is greater for $CD5^{hi}$ T cells than for $CD5^{lo}$ T cells (Palmer et al., 2011). However this death rate does not depend on the level of IL7R expression (see Figure 5). The death rate is switched on if IL7 availability is below a given survival threshold and equivalently, it is switched off if the concentration of IL7 is above this threshold (Palmer et al., 2011). Similarly, if the concentration of IL7 is above a given proliferation threshold, we turn on a proliferation term for $IL7R^{hi}$ T cells. Following a division event $IL7R^{hi}$ T cells produce two daughter cells, in the corresponding $IL7R^{lo}$ pool, in consonance with the altruistic hypothesis. We assume $IL7R^{lo}$ T cells may not receive sufficient IL7 stimulus to undergo a division event. $IL7R^{lo}$ T cells are assumed to upregulate their expression levels of IL7R and become $IL7R^{hi}$ (see Figure 5). Finally, we assume the level of CD5 expression is invariant; that is, $CD5^{hi}$ cells can only increase or decrease their levels of IL7R expression, but maintain their high level of CD5 expression constant. The same is true for $CD5^{lo}$ cells (see Figure 5). The interplay between IL7 receptor expression and signaling on the fate (division, proliferation or IL7R upregulation) of the four different population of $CD8^+$ T cells can be captured mathematically and will be discussed in the following section.

5.3.1 | Mathematical model

We denote by $n_{i,j}$ the number of cells in subset $S_{i,j}$: an index value of "1" always refers to "high," whereas an index of "2" always refers to "low." If a pair of indexes appears in a variable, the first one refers to CD5 and the second to IL7R, respectively. Specifically, we have defined

Cell type	Variable
$CD5^{hi}IL7R^{hi}$	$n_{1,1}$
$CD5^{hi}IL7R^{lo}$	$n_{1,2}$
$CD5^{lo}IL7R^{hi}$	$n_{2,1}$
$CD5^{lo}IL7R^{lo}$	$n_{2,2}$

We now describe the dynamics that characterize the four different population of $CD8^+$ T cells and that are driven by IL7 signaling.

Dynamics of IL7

We model the concentration of IL7 in a deterministic manner, as we argued above. Let I denote the concentration of IL7. We assume IL7 is produced at a constant rate ν, independent of its extracellular level (Kim et al., 2011; Martin et al., 2017). We also consider IL7 loss, due to internalization of IL7 once it binds IL7R expressed on the surface of T cells. We, thus, assume that this loss term is proportional to the global concentration of IL7 and the number of T cells. These terms then take the form

$$-\gamma_1\left(n_{1,1}+n_{2,1}\right)I-\gamma_2\left(n_{1,2}+n_{2,2}\right)I,$$

where $\gamma_1 > \gamma_2$, since we assume $IL7R^{hi}$ cells internalize IL7 at a faster rate than $IL7R^{lo}$ cells, since their IL7R surface expression levels are higher by construction. The concentration of IL7 then obeys an ODE of the form

$$\frac{dI}{dt}=\nu-\gamma_1\left(n_{1,1}+n_{2,1}\right)I-\gamma_2\left(n_{1,2}+n_{2,2}\right)I. \tag{11}$$

Dynamics of T cells

The populations of $CD8^+$ T cells are modeled in a stochastic fashion. Let us introduce a threshold for survival θ_s and a threshold for proliferation θ_p (Palmer et al., 2011; Reynolds et al., 2013). We shall assume the dimensions of θ_s and θ_p to be those of I, that is, volume concentration. We assume that the survival threshold is lower than the proliferation one (Reynolds et al., 2013); that is, $\theta_s < \theta_p$. We now describe the $CD8^+$ T cell dynamics, as follows:

- If $I < \theta_s$ (death event): $n_{i,\,j} \to n_{i,\,j} - 1$, in a small time interval, Δt, with probability $\mu_i\, n_{i,\,j}\, \Delta t$ for $i, j = 1, 2$.
- If $\theta_s < I < \theta_p$ (survival event): $n_{i,\,j} \to n_{i,\,j}$, in a small time interval, Δt, with probability one for $i, j = 1, 2$.
- If $\theta_p < I$ (proliferation event): $\left.\begin{matrix} n_{i,1} \to n_{i,1} - 1 \\ n_{i,2} \to n_{i,2} + 2 \end{matrix}\right\}$ in a small time interval, Δt, with probability $\lambda_i\, n_{i,\,1}\, \Delta t$ for $i = 1, 2$.

- Finally, and given that the upregulation of IL7R is independent of the concentration of IL7, this transition takes the form:
$$\left.\begin{array}{l} n_{i,2} \rightarrow n_{i,2} - 1 \\ n_{i,1} \rightarrow n_{i,1} + 1 \end{array}\right\} \text{ in a small time interval, } \Delta t, \text{ with probability } \phi_i \, n_{i,2} \, \Delta t \text{ for } i = 1, 2.$$

These transitions are illustrated in Figure 5.

Threshold function

We assume the probabilities of death and proliferation events to be nonzero only when the concentration of IL7 is below or above the respective threshold functions for survival and proliferation. The existence of these survival and proliferation thresholds have been experimentally observed (Palmer et al., 2011). We, therefore, choose a function such that when the concentration is above or below a certain threshold, it is either 0 or 1. One such suitable function is the logistic function, defined as follows:

$$f_s(I) = \frac{1}{1 + e^{\alpha(I - \theta_s)}} \qquad \text{and} \qquad f_p(I) = \frac{1}{1 + e^{\alpha(\theta_p - I)}}. \tag{12}$$

We choose the dimensions of α to be inverse concentration, such that the value of $f_s(I)$ is a dimensionless quantity bounded between 0 and 1. This threshold function is then included within the previously defined transition probabilities for death and proliferation events. If $f_\bullet(I) \approx 0$, then the probability of the given event is close to zero and the event is effectively turned off. Similarly if $f_\bullet(I) \approx 1$, then the probability of the event is turned on.

The parameter α modulates the *severity* of the threshold function. In particular, if $\alpha \rightarrow +\infty$, the threshold is extremely sharp. In fact, we have

$$\lim_{\alpha \rightarrow +\infty} f_s(I) = \lim_{\alpha \rightarrow +\infty} \frac{1}{1 + e^{\alpha(I - \theta_s)}} = \begin{cases} 0 & \text{if } I > \theta_s, \\ 1/2 & \text{if } I = \theta_s, \\ 1 & \text{if } I < \theta_s. \end{cases}$$

In Figure 6, we show the threshold functions (see Equation (12)) for different values of α. In the limit $\alpha \rightarrow 0^+$, the thresholds disappear and T cell proliferation and death events do not depend on the amount of free IL7 available. On the other hand, in the limit $\alpha \rightarrow +\infty$ the

5.3.2 | Numerical results

We have implemented the model discussed in Section 5.3.1, making use of a deterministic characterization (ODE) for the concentration of IL7, $I(t)$, and either an ODE model for the number of cells in each *compartment* or a stochastic Markov description, which requires the implementation of a Gillespie algorithm (see code provided in Appendix B). The deterministic model for the four T cell populations and the concentration of IL7 is described in the code provided in Appendix C. The parameters used in the numerical studies have been summarized in Table 3. When other parameter values have been used, we have provided their values explicitly. To model different extracellular signaling environments, describing different values of extracellular IL7 concentration, we vary the value of the parameter ν, and make use of a *soft* threshold given by $\alpha = 5$. As shown in Figures 7–9, different values of ν change the steady state of the four T cell populations. In all cases, on the right

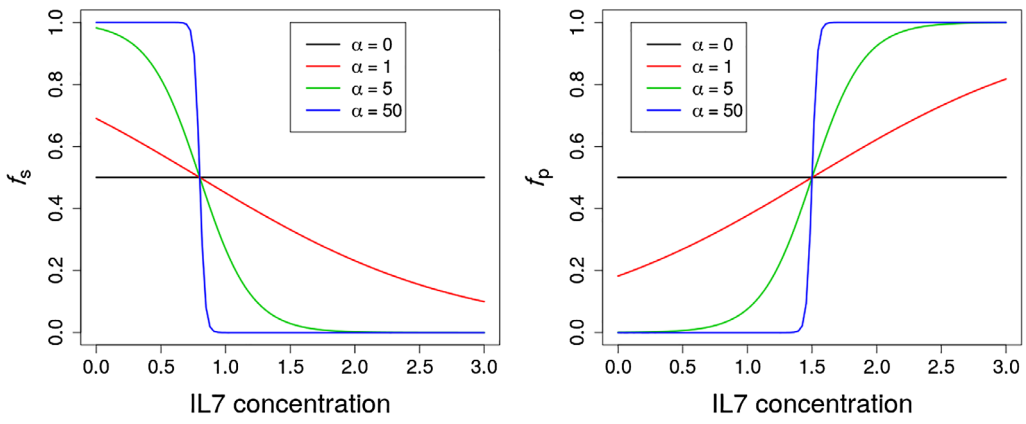

FIGURE 6 Effect of the parameter α on the severity of the threshold functions (see Equation (12)). Note that for $\alpha = 0$ (black line) the threshold functions are constant and equal to $\frac{1}{2}$. On the other hand, for $\alpha \gg 1$ the functions are almost discontinuous and the thresholds rather sharp

TABLE 3 Parameters for the population model of IL7-mediated signaling

Parameter	Value	Units	Reference
$I(0)$	1	[con]	Note 1
$n_{1,\,1}(0)$	50	cells	This work
$n_{1,\,2}(0)$	50	cells	This work
$n_{2,\,1}(0)$	50	cells	This work
$n_{2,\,2}(0)$	50	cells	This work
ν	50	$[\text{con}]^{-1}$ hour^{-1}	Note 2 Reynolds et al. (2013)
γ_1	0.08	hour^{-1}	Reynolds et al. (2013)
γ_2	0.02	hour^{-1}	Chosen to be $\sim \gamma_1/4$
μ_1	0.027	hour^{-1}	Reynolds et al. (2013)
μ_2	0.018	hour^{-1}	Chosen to be $= 2\,\mu_1/3$
λ_1	0.083	hour^{-1}	Reynolds et al. (2013)
λ_2	0.055	hour^{-1}	Chosen to be $= 2\lambda_1/3$
ϕ_1	0.083	hour^{-1}	Chosen to be $= \lambda_1$
ϕ_2	0.042	hour^{-1}	Chosen to be $\sim \phi_1/2$
θ_s	0.8	[con]	This work
θ_p	1.5	[con]	This work
α	5	$[\text{con}]^{-1}$	Note 3
δ	20	h^{-1}	Reynolds et al. (2013)

Note 1: we normalize the initial concentration of IL7 to 1. This allows us to use generic units of concentration ([con]) rather than the standard M (moles/litre). Note 2: we have normalized ν from Reynolds et al. (2013) according to Note 1. Note 3: in order to guarantee a threshold-like response, we have chosen a relatively large value of α.

panel we show the relative number of T cells with high (black lines) and low (red lines) expression of CD5. In that panel we also show two different stochastic simulations to emphasize the role of fluctuations when the number of cells is small (in all cases we have considered that, initially, there is a total of 200 cells, equally distributed between the four compartments). For completeness, in Figure 10 we consider the case where IL7 is removed from the system not only by IL7 receptor-mediated internalization but by other mechanisms (that we denote generically, *degradation*), for the same parameter values as those of Figure 9. Note that, while the maximum level of IL7 changes significantly, the dynamics of the $CD8^+$ T cell populations does not qualitatively change.

From these numerical studies, two significant conclusions can be derived. First of all, different values of ν (the parameter that encodes the IL7 extracellular environment) lead to different relative fractions of cells with high and low expression of CD5. These results are in agreement with the experimental evidence summarized by Palmer et al. (2011). These authors observed population dominance in favor of $CD5^{hi}$ $CD8^+$ T cells in high IL7 environments. In contrast, $CD5^{lo}$ $CD8^+$ T cells were observed to dominate the T cell repertoire in low IL7 environments. In between these, at physiological levels of IL7, an

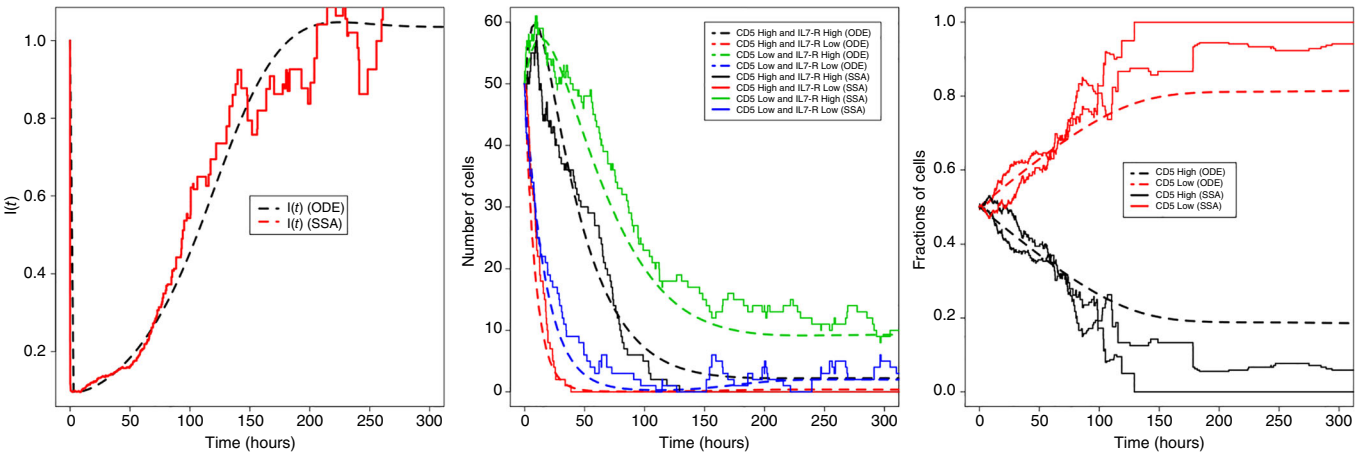

FIGURE 7 Numerical study for a total time of 2 weeks with low IL7 production, $\nu = 1$ and a *soft* threshold, $\alpha = 5$. On the right plot, we see the T cell population is dominated by the subset of $CD5^{lo}$ T cells. Note the reasonable agreement between the deterministic model (ODE) and the stochastic simulations (SSA). On the left plot, we follow the extracellular IL7 concentration in time. On the middle plot, we follow the four cellular populations in time. On the right plot, we follow the two cellular populations, as defined by their CD5 expression in time

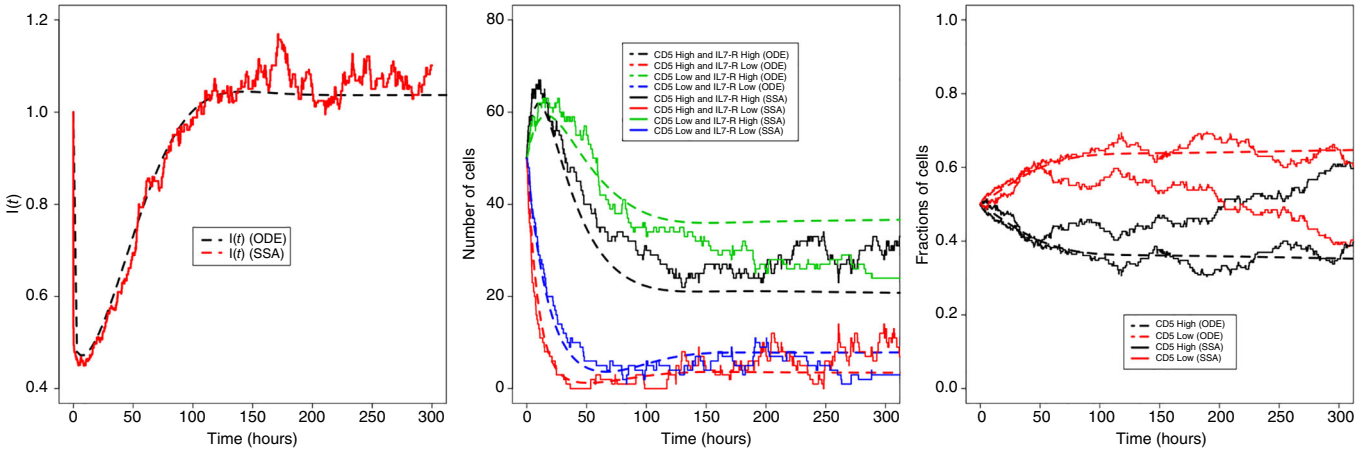

FIGURE 8 Numerical study for a total time of 2 weeks with medium IL7 production, $\nu = 5$ and a *soft* threshold, $\alpha = 5$. On the right plot, we see the T cell population is dominated by the subset of $CD5^{lo}$ T cells. Note that a deterministic (ODE) approach cannot precisely reproduce the stochastic behavior (SSA). On the left plot, we follow the extracellular IL7 concentration in time. On the middle plot, we follow the four cellular populations in time. On the right plot, we follow the two cellular populations, as defined by their CD5 expression in time

equal balance in the T cell repertoire was observed (Palmer et al., 2011). Second, the striking result that the deterministic approximation (ODE) cannot capture the *switch* between low and high IL7 extracellular environments occurring for intermediate values of ν (see, for instance, the right panel in Figure 8). This discrepancy between the deterministic and the stochastic descriptions raises a potential methodological concern; namely, how to choose the value of α. We note that these differences originate from two possible effects: the value of ν and that of α. The first effect is easier to understand, since very large values of ν (see, for instance, Figure 9) drive the cytokine concentration, I, to its deterministic value and stochastic fluctuations are damped out quickly (compare the left plots of Figure 7 and Figure 8 to the left plot of Figure 9). In order to decipher the role of α, we first note that when $\alpha = 0$, the T cell populations do not perceive any IL7 threshold behavior and their dynamics is independent of the amount of free extracellular IL7 available. Second, let us now evaluate the effect of different values of α (and the severity of the thresholds) in the dynamics of the four T cell populations. Figure 11 reproduces the simulations of Figure 8 for $\alpha = 0$ (top) and $\alpha = 50$ (bottom). As discussed above, the case $\alpha = 0$ is not biologically relevant, since the IL7 survival and proliferation thresholds have been observed in experiments (Palmer et al., 2011). Furthermore, for the death and proliferation rates obtained in Reynolds et al. (2013), and in the absence of IL7 survival and proliferation thresholds, the number of T cells increases indefinitely (see middle panel of the top row in Figure 11). Finally, a comparison between the cases $\alpha = 5$ (see Figure 8) and $\alpha = 50$ (see bottom row of Figure 11) shows that sharper threshold functions decrease the size of the stochastic fluctuations.

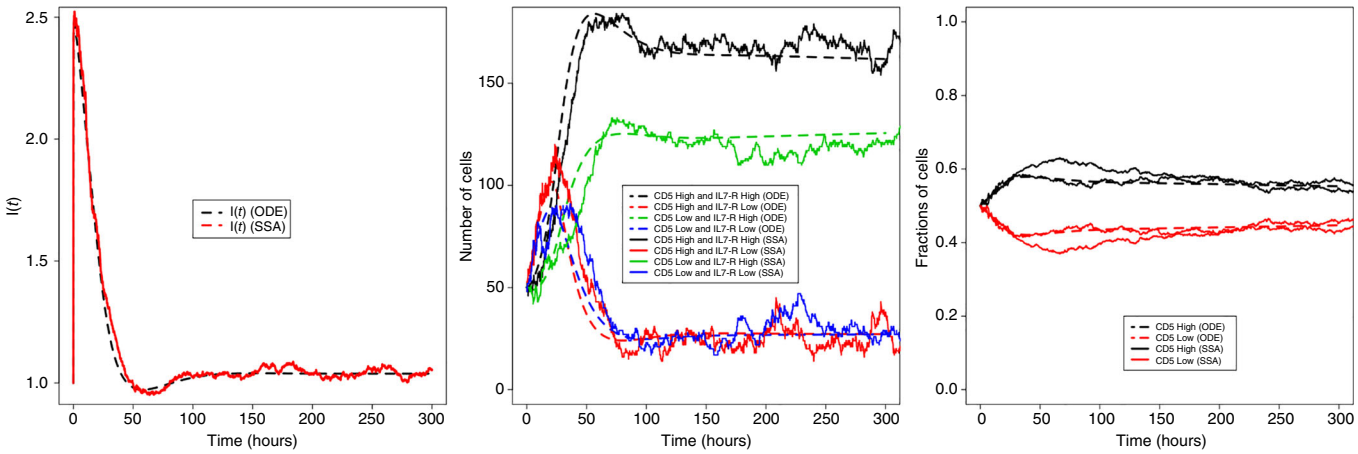

FIGURE 9 Numerical study for a total time of 2 weeks with high IL7 production, $\nu = 25$ and a *soft* threshold, $\alpha = 5$. On the right plot, we see the T cell population is dominated by the subset of $CD5^{hi}$ T cells. Note that a deterministic (ODE) approach is able to reproduce the stochastic behavior (SSA). On the left plot, we follow the extracellular IL7 concentration in time. On the middle plot, we follow the four cellular populations in time. On the right plot, we follow the two cellular populations, as defined by their CD5 expression in time

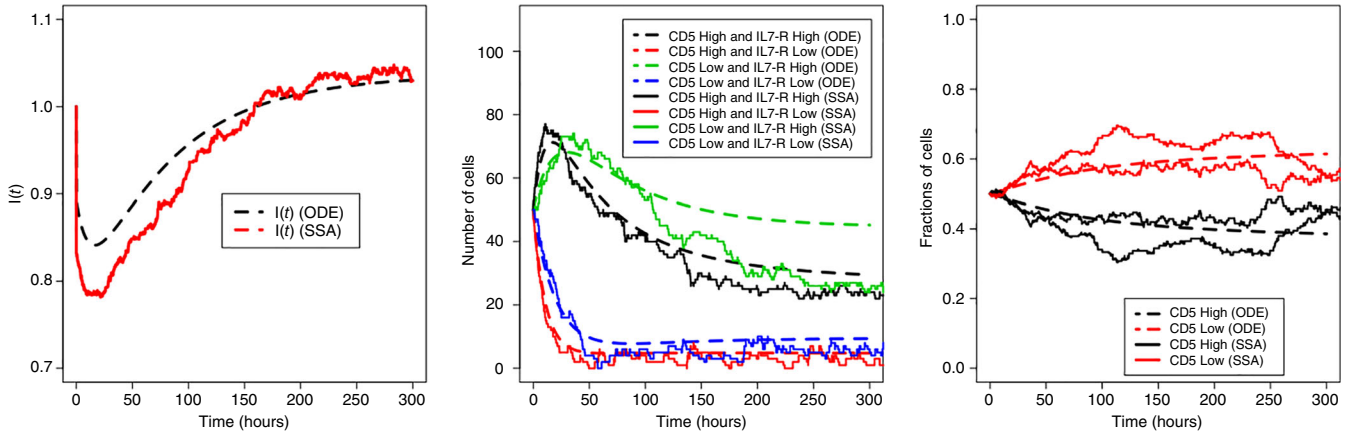

FIGURE 10 Numerical study for a total time of 2 weeks with high IL7 production, $\nu = 25$ and a *soft* threshold, $\alpha = 5$. This study also considers the role of IL7 degradation (with rate $\delta = 20\ \mathrm{h}^{-1}$). On the right plot, we see the T cell population is dominated by the subset of $CD5^{lo}$ T cells. Note that a deterministic (ODE) approach cannot precisely reproduce the stochastic behavior (SSA) observed. On the left plot, we follow the extracellular IL7 concentration in time. On the middle plot, we follow the four cellular populations in time. On the right plot, we follow the two cellular populations, as defined by their CD5 expression in time

In order to further dissect our latter claim, in Figure 12 we show the histogram of stochastic steady states for $\nu = 5$ and for $\alpha = 5$ or $\alpha = 50$. Remarkably, the histogram is so wide that it contains stochastic realizations where there is a switch between the $CD5^{hi}$ and $CD5^{lo}$ populations, which cannot be predicted by the deterministic model. This behavior suggests that, the

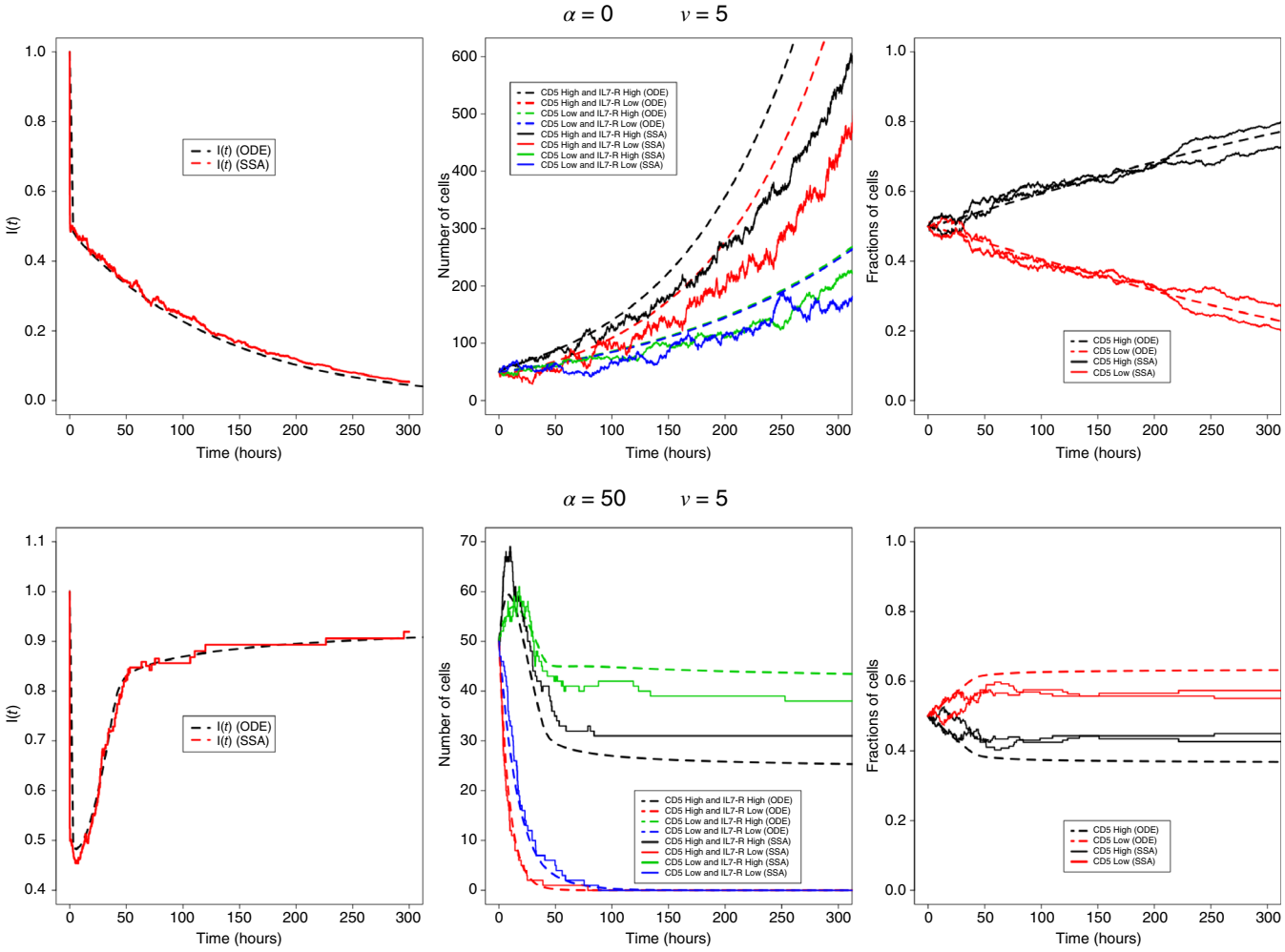

FIGURE 11 Numerical study for a total time of 2 weeks with high IL7 production, $\nu = 5$ for two values of α: $\alpha = 0$ (top row) and $\alpha = 50$ (bottom row). On the left plot, we follow the extracellular IL7 concentration in time. On the middle plot, we follow the four cellular populations in time. On the right plot, we follow the two cellular populations, as defined by their CD5 expression in time

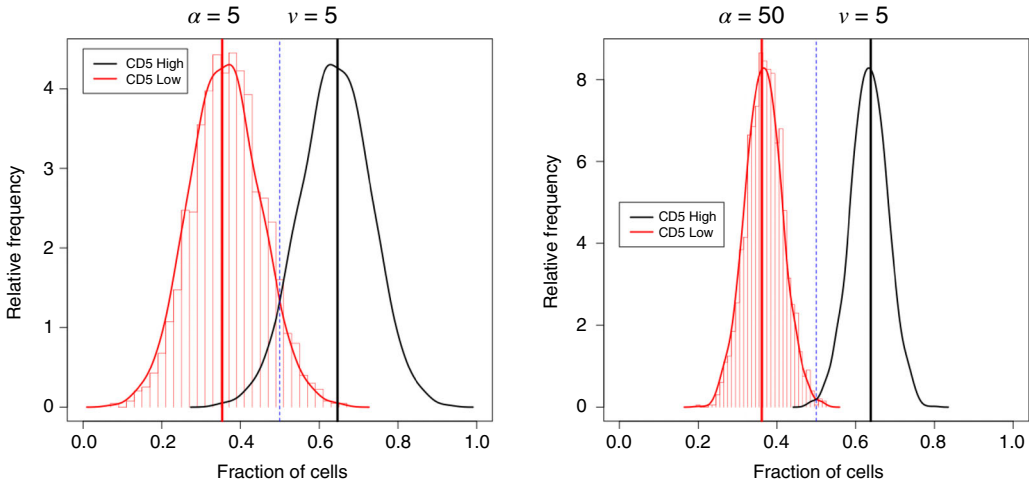

FIGURE 12 Histogram of the steady state of CD5 high subpopulation (black) and CD5 low subpopulation (red) for $\nu = 5$ and $\alpha = 5$ (left) or $\alpha = 50$ (right). The blue dashed vertical line is a guide to the eye to show the line where the fraction of each subpopulation is 50%

combination of nonlinearities (in our case the threshold functions) and a stochastic description, leads to richer outcomes than traditional deterministic approaches. It is beyond the scope of this manuscript to study in greater depth the interplay between stochasticity and threshold responses. Yet, we feel this interplay deserves further analysis since it has not been comprehensively addressed in the literature.

6 | DYSREGULATION OF IL7 RECEPTOR EXPRESSION AND SIGNALING IN CANCER AND INFLAMMATION

Direct evidence for the importance of understanding IL7R biology comes from clinical settings where dysregulation of IL7R expression or signaling were found to be linked with autoimmune inflammatory diseases and tumourigenesis (Dooms, 2013; Tal, Shochat, Geron, Bercovich, & Izraeli, 2014). Both gain- and loss-of-function mutations in the IL7Rα gene have been reported, and there are strong associations between dysregulation of IL7R expression and multiple inflammatory diseases, but also cancer (Mazzucchelli, Riva, & Durum, 2012; Watanabe et al., 1998). Along these lines, about 10% of pediatric T-ALL patients displayed gain-of-function mutations in IL7Rα, which caused ligand-independent activation and signaling of IL7R (Kim, Chung, Kim, Yoo, & Lee, 2013; Ribeiro, Melão, & Barata, 2013; Zenatti et al., 2011). Most of these mutations were found in exon 6 of the IL7Rα gene, at sites that corresponded to the membrane-proximal region of the extracellular domain of the receptor. These mutations could cause homo-dimerization of IL7Rα molecules as they introduced, among others, new cysteine residues which could form disulfide linkage with other mutated IL7Rα proteins. Remarkably, in these tumor cells, IL7Rα homo-dimerization was sufficient to induce ligand-independent IL7Rα signaling, resulting in constitutive STAT5 phosphorylation and activation (Zenatti et al., 2011). Interestingly, earlier studies indicated that homo-dimerization of IL7Rα could not trigger IL7R signaling and that signaling required hetero-dimerization with γ_c receptors, presumably because JAK1 activation required the trans-phosphorylation by JAK3 (Rochman et al., 2009). Why and how IL7Rα mutations in ALL tumor cells can induce productive signaling by IL7Rα homo-dimerization is an intense area of research, and insights from structural biology in conjunction with mathematical modeling are expected to shed light on these open and challenging questions.

As a potential explanation, a recent study suggested the role for IL7Rα trans-membrane domains in the spatial reorganization of mutant IL7Rα homo-dimeric proteins (Shochat et al., 2014). Under normal circumstances, IL7Rα homodimers would dimerise into a configuration where the intracellular domains would all face the same direction and JAK1 molecules would not be juxta-positioned and face each other for trans-phosphorylation. In some IL7Rα mutants, however, twists in the trans-membrane domain would cause rotations of the intracellular region which would position JAK1 molecules into the correct orientation for trans-phosphorylation and activation (Durum, 2014).

Beyond the implications in tumor biology, these findings raise many challenging questions, such as why persistent IL7R signaling would not suppress expression of the oncogenic IL7Rα and how mutant IL7Rα expression would affect conventional IL7Rα signaling, for example. In parallel to biochemical and cellular approaches, we suggest exploiting the power of mathematical and computational modeling, as presented in this review, to enhance our quantitative understanding of these complex immune signaling problems.

7 | DISCUSSION

This review is based on the hypothesis that the development of suitable mathematical models of immune signaling and receptor trafficking will allow us to provide answers to some current health-related challenges: how does the expression level (or its copy number) of a given protein in an immune receptor signaling pathway (or network) affect the type and timescale of cellular responses and how does ligand concentration or protein competition for binding sites on immune receptors drive different cellular fates by turning on/off different intracellular mechanisms, such as endocytosis, degradation, recycling or protein synthesis. From a mathematical perspective, the challenge is to develop a quantitative approach to how receptor-ligand signaling regulates cellular fate that (a) integrates a wide range of molecular, cellular and population data, and (b) improves our understanding of the mechanisms that are dysregulated in disease, so that the mathematical models are accurate predictors of response to receptor-targeted therapies and can aid the design of novel drugs. In this regard, the ability to synthetically create ligands (referred to as synthekines (Moraga et al., 2017)), with the ability to bring together receptor chains that are not naturally paired together, opens a door to novel ways to tune immune signaling. For instance, a dimeric compound of IL7 and IL15 (referred to as IL7.15 in Figure 1), with the ability to bring together IL7Rα with IL15Rβ, can modulate IL7R and IL15R signaling, and thus T cell behavior. Our belief is that mathematical modeling can help quantify, and even predict, the extent of this immune signaling modulation as a function of IL7 and IL15 extracellular concentration.

In the last decade a lot of quantitative work has supported the view that IL7 and its receptor, IL7R, are one of the master regulators of T cell homeostasis (Mazzucchelli & Durum, 2007; Takada & Jameson, 2009). Still a number of questions remain open, as discussed in this review. One of these challenges relates to intracellular events that take place once IL7R has been internalized. While much of the emphasis is often placed at the ligand-receptor level, trafficking, degradation, recycling and receptor synthesis are crucial to understanding how receptor-mediated signaling regulates immune cell fate. Thus, there is a need to develop mathematical models of immune signaling that incorporate receptor trafficking events (de la Higuera et al., 2017; Reynolds et al., 2013). Recent experimental advances (Freed et al., 2017) together with novel mathematical models will be essential to enhance our understanding of the mechanisms that regulate receptor-mediated immune signaling, and in turn will allow us to decipher how signaling determines immune cellular fate.

Finally, in this review we have presented a number of mathematical models, each of them at a different level of description (molecular, cellular and population, respectively). A current challenge and opportunity for applied mathematics is to integrate the different scales involved in the biological system under consideration. In this direction, agent-based models (Castro, Lythe, & Molina-París, 2017) are good candidates, as they bring together the characteristics of single cells with the dynamics of the whole population. Agent-based models, in combination with traditional mathematical models (based for instance in ODEs, as we discussed in Section 5.3), enable us to integrate different timescales.

We conclude with a reference to some recent work which has highlighted the relevance and significance of mathematical modeling in Immunology (Castro, Lythe, Molina-París, & Ribeiro, 2016). This latter reference has collected a number of studies of T cell immunology to illustrate the benefits of theoretical and experimental collaborations, not only at the receptor and signaling level, as we have done in this review.

ACKNOWLEDGMENTS

This work has been supported by the Intramural Research Program of the Center for Cancer Research, NCI, NIH, and by grants FIS2016-78883-C2-2-P and PRX 16/00287 (MC) from the Spanish Ministry of Economy (MINECO), the European Union FP7 Programme under agreement PIRSES-GA-2012-317893 (MC and CMP), and the European Union H2020 Programme under agreement 764698 MSCA-ITN-2017 (QuanTII ETN) (CMP). CMP dedicates this paper to the memory of Robin Callard. Robin was essential in her transition from theoretical physics to mathematical immunology. We lost him too early and we shall miss him!

CONFLICT OF INTEREST

The authors have declared no conflicts of interest for this article.

ENDNOTE

[1]If the intracellular levels of the potential transcription factor, m_4, are such that $m_4 \gg \kappa_s$, the synthesis rate is considerably reduced.

RELATED WIREs ARTICLE

Rule-based modeling: A computational approach for studying biomolecular site dynamics in cell signaling systems

REFERENCES

Abe, A., Tani-ichi, S., Shitara, S., Cui, G., Yamada, H., Miyachi, H., … Ikuta, K. (2015). An enhancer of the il-7 receptor α-chain locus controls il-7 receptor expression and maintenance of peripheral t cells. *The Journal of Immunology*, *195*(7), 3129–3138.

Akashi, K., Kondo, M., von Freeden-Jeffry, U., Murray, R., & Weissman, I. L. (1997). Bcl-2 rescues t lymphopoiesis in interleukin-7 receptor–deficient mice. *Cell*, *89*(7), 1033–1041.

Blinov, M. L., Faeder, J. R., Goldstein, B., & Hlavacek, W. S. (2004). Bionetgen: Software for rule-based modeling of signal transduction based on the interactions of molecular domains. *Bioinformatics*, *20*(17), 3289–3291.

Busse, D., de la Rosa, M., Hobiger, K., Thurley, K., Flossdorf, M., Scheffold, A., & Höfer, T. (2010). Competing feedback loops shape il-2 signaling between helper and regulatory t lymphocytes in cellular microenvironments. *Proceedings of the National Academy of Sciences of the United States of America*, *107*(7), 3058–3063.

Callard, R., George, A. J. T., & Stark, J. (1999). Cytokines, chaos, and complexity. *Immunity*, *11*(5), 507–513.

Castro, M., Lythe, G., & Molina-París, C. (2017). The t cells in an ageing virtual mouse. In *Stochastic processes, multiscale modeling, and numerical methods for computational cellular biology* (pp. 127–140). New York: Springer.

Castro, M., Lythe, G., Molina-París, C., & Ribeiro, R. M. (2016). Mathematics in modern immunology. *Interface Focus*, *6*(2), 20150093.

Chong, M. M. W., Cornish, A. L., Darwiche, R., Stanley, E. G., Purton, J. F., Godfrey, D. I., … Kay, T. W. H. (2003). Suppressor of cytokine signaling-1 is a critical regulator of interleukin-7-dependent cd8+ t cell differentiation. *Immunity*, *18*(4), 475–487.

Cotari, J. W., Voisinne, G., Dar, O. E., Karabacak, V., & Altan-Bonnet, G. (2013). Cell-to-cell variability analysis dissects the plasticity of signaling of common γ chain cytokines in t cells. *Science Signaling*, *6*(266), ra17–ra17.

de la Higuera, L., López-García, M., Lythe, G., & Molina-París, C. (2017). Il-2 stimulation of regulatory t cells: A stochastic and algorithmic approach. In *Modeling cellular systems* (pp. 81–105). New York: Springer.

DeKoter, R. P., Lee, H.-J., & Singh, H. (2002). Pu. 1 regulates expression of the interleukin-7 receptor in lymphoid progenitors. *Immunity*, *16*(2), 297–309.

Depper, J. M., Leonard, W. J., Drogula, C., Krönke, M., Waldmann, T. A., & Greene, W. C. (1985). Interleukin 2 (il-2) augments transcription of the il-2 receptor gene. *Proceedings of the National Academy of Sciences of the United States of America*, *82*(12), 4230–4234.

Dooms, H. (2013). Interleukin-7: Fuel for the autoimmune attack. *Journal of Autoimmunity*, *45*, 40–48.

Durum, S. K. (2014). Il-7 and tslp receptors: Twisted sisters. *Blood*, *124*(1), 4–5.

Faeder, J. R., Blinov, M. L., & Hlavacek, W. S. (2009). Rule-based modeling of biochemical systems with bionetgen. *Systems Biology*, *500*, 113–167.

Faller, E. M., Ghazawi, F. M., Cavar, M., & MacPherson, P. A. (2016). Il-7 induces clathrin-mediated endocytosis of cd127 and subsequent degradation by the proteasome in primary human cd8 t cells. *Immunology and Cell Biology*, *94*(2), 196–207.

Fallon, E. M., & Lauffenburger, D. A. (2000). Computational model for effects of ligand/receptor binding properties on interleukin-2 trafficking dynamics and t cell proliferation response. *Biotechnology Progress*, *16*(5), 905–916.

Feinerman, O., Jentsch, G., Tkach, K. E., Coward, J. W., Hathorn, M. M., Sneddon, M. W., … Altan-Bonnet, G. (2010). Single-cell quantification of il-2 response by effector and regulatory t cells reveals critical plasticity in immune response. *Molecular Systems Biology*, *6*(1), 437.

Feng, X., Wang, H., Takata, H., Day, T. J., Willen, J., & Hu, H. (2011). Transcription factor foxp1 exerts essential cell-intrinsic regulation of the quiescence of naive t cells. *Nature Immunology*, *12*(6), 544–550.

Fredriksson, S., Gullberg, M., Jarvius, J., Olsson, C., Pietras, K., Gústafsdóttir, S. M., … Landegren, U. (2002). Protein detection using proximity-dependent dna ligation assays. *Nature Biotechnology*, *20*(5), 473–477.

Freed, D. M., Bessman, N. J., Kiyatkin, A., Salazar-Cavazos, E., Byrne, P. O., Moore, J. O., … Lemmon, M. A. (2017). Egfr ligands differentially stabilize receptor dimers to specify signaling kinetics. *Cell*, *171*(3), 683–695.

Friedrich, C., & Gasteiger, G. (2017). Ilcs and t cells competing for space: More than a numbers game. *Immunity*, *47*(1), 8–10.

Fry, T. J., Connick, E., Falloon, J., Lederman, M. M., Liewehr, D. J., Spritzler, J., … Mackall, C. L. (2001). A potential role for interleukin-7 in t-cell homeostasis. *Blood*, *97*(10), 2983–2990.

Fry, T. J., & Mackall, C. L. (2002). Interleukin-7: From bench to clinic. *Blood*, *99*(11), 3892–3904.

Gonnord, P., Angermann, B. R., Sadtler, K., Gombos, E., Chappert, P., Meier-Schellersheim, M., & Varma, R. (2018). A hierarchy of affinities between cytokine receptors and the common gamma chain leads to pathway cross-talk. *Science Signaling*, *11*(524), eaal1253.

Henriques, C. M., Rino, J., Nibbs, R. J., Graham, G. J., & Barata, J. T. (2010). Il-7 induces rapid clathrin-mediated internalization and jak3-dependent degradation of il-7rα in t cells. *Blood*, *115*(16), 3269–3277.

Hong, C., Luckey, M. A., Ligons, D. L., Waickman, A. T., Park, J.-Y., Kim, G. Y., … Park, J.-H. (2014). Activated t cells secrete an alternatively spliced form of common γ-chain that inhibits cytokine signaling and exacerbates inflammation. *Immunity*, *40*(6), 910–923.

Jiang, Q., Li, W. Q., Hofmeister, R. R., Young, H. A., Hodge, D. R., Keller, J. R., … Durum, S. K. (2004). Distinct regions of the interleukin-7 receptor regulate different bcl2 family members. *Molecular and Cellular Biology*, *24*(14), 6501–6513.

Katz, G., Pobezinsky, L. A., Jeurling, S., Shinzawa, M., Van Laethem, F., & Singer, A. (2014). T cell receptor stimulation impairs il-7 receptor signaling by inducing expression of the microrna mir-17 to target janus kinase 1. *Science Signaling*, *7*(340), ra83–ra83.

Kerdiles, Y. M., Beisner, D. R., Tinoco, R., Dejean, A. S., Castrillon, D. H., DePinho, R. A., & Hedrick, S. M. (2009). Foxo1 links homing and survival of naive t cells by regulating l-selectin, ccr7 and interleukin 7 receptor. *Nature Immunology*, *10*(2), 176–184.

Kim, G. Y., Hong, C., & Park, J.-H. (2011). Seeing is believing: Illuminating the source of in vivo interleukin-7. *Immune Network*, *11*(1), 1–10.

Kim, K., Lee, C.-k., Sayers, T. J., Muegge, K., & Durum, S. K. (1998). The trophic action of il-7 on pro-t cells: Inhibition of apoptosis of pro-t1,-t2, and-t3 cells correlates with bcl-2 and bax levels and is independent of fas and p53 pathways. *The Journal of Immunology*, *160*(12), 5735–5741.

Kim, M. S., Chung, N. G., Kim, M. S., Yoo, N. J., & Lee, S. H. (2013). Somatic mutation of il7r exon 6 in acute leukemias and solid cancers. *Human Pathology*, *44*(4), 551–555.

Kimura, M. Y., Pobezinsky, L. A., Guinter, T. I., Thomas, J., Adams, A., Park, J.-H., … Singer, A. (2013). Il-7 signaling must be intermittent, not continuous, during cd8+ t cell homeostasis to promote cell survival instead of cell death. *Nature Immunology*, *14*(2), 143–151.

Lee, H.-C., Shibata, H., Ogawa, S., Maki, K., & Ikuta, K. (2005). Transcriptional regulation of the mouse il-7 receptor α promoter by glucocorticoid receptor. *The Journal of Immunology*, *174*(12), 7800–7806.

Ligons, D. L., Tuncer, C., Linowes, B. A., Akcay, I. M., Kurtulus, S., Deniz, E., … Park, J.-H. (2012). Cd8 lineage-specific regulation of interleukin-7 receptor expression by the transcriptional repressor gfi1. *Journal of Biological Chemistry*, *287*(41), 34386–34399.

Liu, W., Putnam, A. L., Xu-Yu, Z., Szot, G. L., Lee, M. R., Zhu, S., … Bluestone, J. A. (2006). Cd127 expression inversely correlates with foxp3 and suppressive function of human cd4+ t reg cells. *Journal of Experimental Medicine*, *203*(7), 1701–1711.

Luckey, M. A., Kimura, M. Y., Waickman, A. T., Feigenbaum, L., Singer, A., & Park, J.-H. (2014). The transcription factor thpok suppresses runx3 and imposes cd4+ lineage fate by inducing the socs suppressors of cytokine signaling. *Nature immunology*, *15*(7), 638–645.

Marino, J. H., Tan, C., Taylor, A. A., Bentley, C., Van De Wiele, C. J., Ranne, R., … Teague, T. K. (2010). Differential il-7 responses in developing human thymocytes. *Human immunology*, *71*(4), 329–333.

Martin, C. E., Spasova, D. S., Frimpong-Boateng, K., Kim, H.-O., Lee, M., Kim, K. S., & Surh, C. D. (2017). Interleukin-7 availability is maintained by a hematopoietic cytokine sink comprising innate lymphoid cells and t cells. *Immunity*, *47*(1), 171–182.

Mazzucchelli, R., & Durum, S. K. (2007). Interleukin-7 receptor expression: Intelligent design. *Nature Reviews Immunology*, *7*(2), 144–154.

Mazzucchelli, R. I., Riva, A., & Durum, S. K. (2012). The human il-7 receptor gene: Deletions, polymorphisms and mutations. *Seminars in Immunology*, *24*, 225–230.

McCaughtry, T. M., Etzensperger, R., Alag, A., Tai, X., Kurtulus, S., Park, J.-H., … Singer, A. (2012). Conditional deletion of cytokine receptor chains reveals that il-7 and il-15 specify cd8 cytotoxic lineage fate in the thymus. *Journal of Experimental Medicine*, *209*(12), 2263–2276.

McElroy, C. A., Holland, P. J., Zhao, P., Lim, J.-M., Wells, L., Eisenstein, E., & Walsh, S. T. R. (2012). Structural reorganization of the interleukin-7 signaling complex. *Proceedings of the National Academy of Sciences of the United States of America*, *109*(7), 2503–2508.

Moraga, I., Spangler, J. B., Mendoza, J. L., Gakovic, M., Wehrman, T. S., Krutzik, P., & Christopher Garcia, K. (2017). Synthekines are surrogate cytokine and growth factor agonists that compel signaling through non-natural receptor dimers. *eLife*, *6*, e22882.

Munitic, I., Williams, J. A., Yang, Y., Dong, B., Lucas, P. J., El Kassar, N., … Ashwell, J. D. (2004). Dynamic regulation of il-7 receptor expression is required for normal thymopoiesis. *Blood*, *104*(13), 4165–4172.

Noguchi, M., Nakamura, Y., Russell, S. M., Ziegler, S. F., Tsang, M., Cao, X., & Leonard, W. J. (1993). Interleukin-2 receptor g chain: A functional component of the interleukin-4 receptor. *Science*, *262*, 1877–1880.

Noguchi, M., Sarin, A., Javad Aman, M., Nakajima, H., Shores, E. W., Henkart, P. A., & Leonard, W. J. (1997). Functional cleavage of the common cytokine receptor γ chain (γc) by calpain. *Proceedings of the National Academy of Sciences of the United States of America*, *94*(21), 11534–11539.

Opferman, J. T., Letai, A., Beard, C., Sorcinelli, M. D., Ong, C. C., & Korsmeyer, S. J. (2003). Development and maintenance of b and t lymphocytes requires antiapoptotic mcl-1. *Nature*, *426*(6967), 671–676.

Palmer, M. J., Mahajan, V. S., Chen, J., Irvine, D. J., & Lauffenburger, D. A. (2011). Signaling thresholds govern heterogeneity in il-7-receptor-mediated responses of naive cd8+ t cells. *Immunology and Cell Biology*, *89*(5), 581–594.

Palmer, M. J., Mahajan, V. S., Trajman, L. C., Irvine, D. J., Lauffenburger, D. A., & Chen, J. (2008). Interleukin-7 receptor signaling network: An integrated systems perspective. *Cellular & Molecular Immunology*, *5*(2), 79–89.

Park, J.-Y., Jo, Y., Ko, E., Luckey, M. A., Park, Y. K., Park, S.-H., … Hong, C. (2016). Soluble γc cytokine receptor suppresses il-15 signaling and impairs inkt cell development in the thymus. *Scientific Reports*, *6*, 36962.

Park, J.-H., Adoro, S., Guinter, T., Erman, B., Alag, A. S., Catalfamo, M., … Singer, A. (2010). Signaling by intrathymic cytokines, not t cell antigen receptors, specifies cd8 lineage choice and promotes the differentiation of cytotoxic-lineage t cells. *Nature Immunology*, *11*(3), 257–264.

Park, J.-H., Qing, Y., Erman, B., Appelbaum, J. S., Montoya-Durango, D., Leighton Grimes, H., & Singer, A. (2004). Suppression of il7rα transcription by il-7 and other prosurvival cytokines: A novel mechanism for maximizing il-7-dependent t cell survival. *Immunity*, *21*(2), 289–302.

Peschon, J. J., Morrissey, P. J., Grabstein, K. H., Ramsdell, F. J., Maraskovsky, E., Gliniak, B. C., … Davison, B. L. (1994). Early lymphocyte expansion is severely impaired in interleukin 7 receptor-deficient mice. *Journal of Experimental Medicine*, *180*(5), 1955–1960.

Raeber, M. E., Zurbuchen, Y., Impellizzieri, D., & Boyman, O. (2018). The role of cytokines in t-cell memory in health and disease. *Immunological Reviews*, *283*(1), 176–193.

Rathmell, J. C., Farkash, E. A., Gao, W., & Thompson, C. B. (2001). Il-7 enhances the survival and maintains the size of naive t cells. *The Journal of Immunology*, *167*(12), 6869–6876.

Reynolds, J., Coles, M., Lythe, G., & Molina-París, C. (2013). Mathematical model of naive t cell division and survival il-7 thresholds. *Frontiers in Immunology*, *4*, 434.

Ribeiro, D., Melão, A., & Barata, J. T. (2013). Il-7r-mediated signaling in t-cell acute lymphoblastic leukemia. *Advances in Biological Regulation*, *53*(2), 211–222.

Rochman, Y., Spolski, R., & Leonard, W. J. (2009). New insights into the regulation of t cells by γc family cytokines. *Nature Reviews Immunology*, *9*(7), 480–490.

Rose, T., Pillet, A.-H., Lavergne, V., Tamarit, B., Lenormand, P., Rousselle, J.-C., … Thèze, J. (2010). Interleukin-7 compartmentalizes its receptor signaling complex to initiate cd4 t lymphocyte response. *Journal of Biological Chemistry*, *285*(20), 14898–14908.

Schluns, K. S., Kieper, W. C., Jameson, S. C., & Lefrançois, L. (2000). Interleukin-7 mediates the homeostasis of naive and memory cd8 t cells in vivo. *Nature Immunology*, *1*(5), 426–432.

Sekar, J. A. P., & Faeder, J. R. (2017). An introduction to rule-based modeling of immune receptor signaling. *arXiv preprint arXiv*, *1709*, 06658.

Shimizu, A., Kondo, S., Sabe, H., Ishida, N., & Honjo, T. (1986). Structure and function of the interleukin 2 receptor: Affinity conversion model. *Immunological Reviews*, *92*(1), 103–120.

Shochat, C., Tal, N., Gryshkova, V., Birger, Y., Bandapalli, O. R., Cazzaniga, G., … Izraeli, S. (2014). Novel activating mutations lacking cysteine in type i cytokine receptors in acute lymphoblastic leukemia. *Blood*, *124*(1), 106–110.

Singer, A., Adoro, S., & Park, J.-H. (2008). Lineage fate and intense debate: Myths, models and mechanisms of cd4-versus cd8-lineage choice. *Nature Reviews Immunology*, *8*(10), 788–801.

Takada, K., & Jameson, S. C. (2009). Naive t cell homeostasis: From awareness of space to a sense of place. *Nature Reviews Immunology*, *9*(12), 823–832.

Tal, N., Shochat, C., Geron, I., Bercovich, D., & Izraeli, S. (2014). Interleukin 7 and thymic stromal lymphopoietin: From immunity to leukemia. *Cellular and Molecular Life Sciences*, *71*(3), 365–378.

Tan, J. T., Dudl, E., LeRoy, E., Murray, R., Sprent, J., Weinberg, K. I., & Surh, C. D. (2001). Il-7 is critical for homeostatic proliferation and survival of naive t cells. *Proceedings of the National Academy of Sciences of the United States of America*, *98*(15), 8732–8737.

Venkitaraman, A. R., & Cowling, R. J. (1994). Interleukin-7 induces the association of phosphatidylinositol 3-kinase with the α chain of the interleukin-7 receptor. *European Journal of Immunology*, *24*(9), 2168–2174.

von Freeden-Jeffry, U., Vieira, P., Lucian, L. A., McNeil, T., Burdach, S. E., & Murray, R. (1995). Lymphopenia in interleukin (il)-7 gene-deleted mice identifies il-7 as a nonredundant cytokine. *Journal of Experimental Medicine*, *181*(4), 1519–1526.

Waickman, A. T., Park, J.-Y., & Park, J.-H. (2016). The common γ-chain cytokine receptor: Tricks-and-treats for t cells. *Cellular and Molecular Life Sciences*, *73*(2), 253–269.

Waldmann, T. A. (2015). The shared and contrasting roles of il2 and il15 in the life and death of normal and neoplastic lymphocytes: Implications for cancer therapy. *Cancer Immunology Research*, *3*(3), 219–227.

Walsh, S. T. R. (2012). Structural insights into the common γ-chain family of cytokines and receptors from the interleukin-7 pathway. *Immunological Reviews*, *250*(1), 303–316.

Watanabe, M., Ueno, Y., Yajima, T., Okamoto, S., Hayashi, T., Yamazaki, M., … Hibi, T. (1998). Interleukin 7 transgenic mice develop chronic colitis with decreased interleukin 7 protein accumulation in the colonic mucosa. *Journal of Experimental Medicine*, *187*(3), 389–402.

Wofford, J. A., Wieman, H. L., Jacobs, S. R., Zhao, Y., & Rathmell, J. C. (2008). Il-7 promotes glut1 trafficking and glucose uptake via stat5-mediated activation of akt to support t-cell survival. *Blood*, *111*(4), 2101–2111.

Xue, H.-H., Bollenbacher, J., Rovella, V., Tripuraneni, R., Du, Y.-B., Liu, C.-Y., … Leonard, W. J. (2004). Ga binding protein regulates interleukin 7 receptor α-chain gene expression in t cells. *Nature Immunology*, *5*(10), 1036–1044.

Yu, Q., Erman, B., Bhandoola, A., Sharrow, S. O., & Singer, A. (2003). In vitro evidence that cytokine receptor signals are required for differentiation of double positive thymocytes into functionally mature cd8+ t cells. *Journal of Experimental Medicine*, *197*(4), 475–487.

Yu, Q., Erman, B., Park, J.-H., Feigenbaum, L., & Singer, A. (2004). Il-7 receptor signals inhibit expression of transcription factors tcf-1, lef-1, and rorγt. *Journal of Experimental Medicine*, *200*(6), 797–803.

Yu, Q., Park, J.-H., Doan, L. L., Erman, B., Feigenbaum, L., & Singer, A. (2006). Cytokine signal transduction is suppressed in preselection double-positive thymocytes and restored by positive selection. *Journal of Experimental Medicine*, *203*(1), 165–175.

Zenatti, P. P., Ribeiro, D., Li, W., Zuurbier, L., Silva, M. C., Paganin, M., … Barata, J. T. (2011). Oncogenic il7r gain-of-function mutations in childhood t-cell acute lymphoblastic leukemia. *Nature Genetics*, *43*(10), 932–939.

How to cite this article: Park J-H, Waickman AT, Reynolds J, Castro M, Molina-París C. IL7 receptor signaling in T cells: A mathematical modeling perspective. *WIREs Syst Biol Med*. 2019;e1447. https://doi.org/10.1002/wsbm.1447

APPENDIX A: CODE LISTING FOR MOLECULAR LEVEL MODEL (SEE SECTION 5.1)

```
begin model

begin parameters
NA 6.02214e23 # molecules per mol (Avogadro constant)
cellDensity 1e11 # cells per L (1e5 cells per uL)
Vecf=1/cellDensity
# concentration of IL-7 at time t=0
dens7 1 # nM (used for parametric plot)
IL7_0 dens7*1.0e-9*(NA*Vecf) # M converted to copies per cell (cpc)
# concentration of IL-15 at time t=0
dens15 0.10 # nM (used for parametric plot)
IL15_0 dens15*1.0e-9*(NA*Vecf) # M converted to copies per cell (cpc)
# number of receptors per cell
IL7Ralpha_0 1.0e3 # cpc
IL15Rbeta_0 1.0e3 # cpc
g0 1.0e3 # (used for parametric plot)
gammac_0 g0 # cpc
# Reaction rates (f: forward/ r: backward)
kf1 1.0e9/(NA*Vecf) # in units of M^{-1} min^{-1} converted to /(molecules/cell)/s
kr1 0.1 # in units of  min^{-1}
kf2 1.0e9/(NA*Vecf) # in units of M^{-1} min^{-1} converted to /(molecules/cell)/s
kr2 0.1 # in units of  min^{-1}
kf3 1.0e9/(NA*Vecf) # in units of M^{-1} min^{-1} converted to /(molecules/cell)/s
kr3 0.1 # in units of  min^{-1}
kf4 0.1*1.0e9/(NA*Vecf) # in units of M^{-1} min^{-1} converted to /(molecules/cell)/s
kr4 0.1 # in units of  min^{-1}
end parameters

begin molecule types
IL7(r,r) # IL-7 (ligand to be bound to receptor site "r" )
IL15(r,r) # IL-15 (ligand to be bound to receptor site "r")
IL7Ralpha(r,l) # IL-7Ralpha receptor (attach to gammac via "r" or ligand via "l")
IL15Rbeta(r,l) # IL-5Rbeta receptor (attach to gammac via "r" or ligand via "l")
gammac(r,l) # gammac (attach to gammac via "r" or ligand via "l")
end molecule types

begin seed species
IL7(r,r) IL7_0
IL15(r,r) IL15_0
IL7Ralpha(r,l) IL7Ralpha_0
IL15Rbeta(r,l) IL15Rbeta_0
gammac(r,l) gammac_0
end seed species

begin observables
Species Bound7R  IL7Ralpha.gammac.IL7
Species Bound15R  IL15Rbeta.gammac.IL15
end observables

begin functions
Fraction7() = Bound7R/(Bound7R+Bound15R)
end functions

begin reaction rules
IL7Ralpha(r,l) + gammac(r,l) <->IL7Ralpha(r!1,l).gammac(r!1,l) kf1,kr1 # heterodimerization
IL15Rbeta(r,l) + gammac(r,l) <->IL15Rbeta(r!1,l).gammac(r!1,l) kf2,kr2 # heterodimerization
# Binding
IL7Ralpha(r!1,l).gammac(r!1,l) + IL7(r,r) <->IL7Ralpha(r!1,l!2).gammac(r!1,l!3).IL7(r!2,r!3) kf3,kf3
IL15Rbeta(r!1,l).gammac(r!1,l) + IL15(r,r) <->IL15Rbeta(r!1,l!2).gammac(r!1,l!3).IL15(r!2,r!3) kf4,kf4
end reaction rules

end model

generate_network({overwrite=>1}); # Generate network

#simulate_ode({t_end=>1000, n_steps=>100,print_functions=>1}); # Get time-course
#parameter_scan({method=>"ode",par_min=>1e-1,par_max=>1e3,\
parameter_scan({method=>"ode",par_min=>1e0,par_max=>1e5,\
                n_scan_pts=>50,log_scale=>1,t_end=>1000,n_steps=>2,print_functions=>1,\
                parameter=>"dens7"}) # Change by dens15 or g0 for Figures 2b-c
```

APPENDIX B: CODE LISTING FOR POPULATION LEVEL STOCHASTIC MODEL (SEE SECTION 5.3)

```
##########################################################################
# Simulation of IL-7 model using Gillespie algorithm and Euler method for
# solution of ODE governing IL-7 dynamics
##########################################################################

import numpy as np, matplotlib.pyplot as plt, math, random

I0 = 1
N1 = 50
N2 = 50
N3 = 50
N4 = 50

gam1 = 0.08
gam2 = 0.02
mu1 = 0.028
mu2 = 0.017
lam1 = 0.083
lam2 = 0.055
phi1 = 0.083
phi2 = 0.042

kap_s = 0.8
kap_p = 1.5
alpha = 5

h = 0.001
dt = 0.01
t_end = 300# 3350 # 72

delta = 0 # h^-1
nu = 50 # 1, 15, 50

n_steps = int(t_end / dt)

def IL7(n1,n2,n3,n4,I):
    return nu - gam1 * (n1 + n3) * I - gam2 * (n2 + n4) * I - delta * I

def rho_s(I):
    return 1 / (1 + math.exp(alpha * (I - kap_s)))

def rho_p(I):
    return 1 / (1 + math.exp(alpha * (kap_p - I)))

X = np.zeros((6,n_steps))

X[0][0] = I0
X[1][0] = N1
X[2][0] = N2
X[3][0] = N3
X[4][0] = N4
X[5][0] = N1+N2+N3+N4

I = I0
n1 = N1
n2 = N2
n3 = N3
n4 = N4
t = 0

IL=[]

for k in range(0,n_steps):
    while t < k*dt:
```

```
        if n1 == 0 and n2 == 0 and n3 == 0 and n4 == 0:
            break
        rmu1 = mu1*n1*rho_s(I)
        rmu2 = mu1*n2*rho_s(I)
        rmu3 = mu2*n3*rho_s(I)
        rmu4 = mu2*n4*rho_s(I)
        rlam1 = lam1*n1*rho_p(I)
        rlam2 = lam2*n3*rho_p(I)
        rphi1 = phi1*n2
        rphi2 = phi2*n4
        rtotal = rmu1+rmu2+rmu3+rmu4+rlam1+rlam2+rphi1+rphi2
        r1 = random.random()
        T = -(1/rtotal) * math.log(r1)
        t += T
        r2 = random.random()
        r2 = r2*rtotal

        if 0 <= r2 < rmu1:
            n1 -= 1
        elif rmu1 <= r2 < rmu1+rmu2:
            n2 -= 1
        elif rmu1+rmu2 <= r2 < rmu1+rmu2+rmu3:
            n3 -= 1
        elif rmu1+rmu2+rmu3 <= r2 < rmu1+rmu2+rmu3+rmu4:
            n4 -= 1
        elif rmu1+rmu2+rmu3+rmu4 <= r2 < rmu1+rmu2+rmu3+rmu4+rlam1:
            n1 -= 1
            n2 += 2
        elif rmu1+rmu2+rmu3+rmu4+rlam1 <= r2 < rmu1+rmu2+rmu3+rmu4+rlam1+rlam2:
            n3 -= 1
            n4 += 2
        elif rmu1+rmu2+rmu3+rmu4+rlam1+rlam2 <= r2 < rmu1+rmu2+rmu3+rmu4+rlam1+rlam2+rphi1:
            n1 += 1
            n2 -= 1
        elif rmu1+rmu2+rmu3+rmu4+rlam1+rlam2+rphi1 <= r2 < rtotal:
            n3 += 1
            n4 -= 1

        n_iter = int(T / h)
        for l in range(0,n_iter):
            I = I + h * IL7(n1,n2,n3,n4,I)
            IL.append(I)

    X[0][k] = I
    X[1][k] = n1
    X[2][k] = n2
    X[3][k] = n3
    X[4][k] = n4
    X[5][k] = n1+n2+n3+n4

xticks = []
tickinterval = t_end / (5*dt)
for k in range(0,6):
    xticks.append(k*tickinterval)
xlabels = []
ticks = t_end / 5
for k in range(0,6):
    xlabels.append(k*ticks)

Ixticks = []
Ixtickint = t_end / (5*h)
for k in range(0,6):
    Ixticks.append(k*Ixtickint)
Ilabels = []
Iticks = t_end / 5
for k in range(0,6):
    Ilabels.append(k*Iticks)
```

```
np.savetxt("concentration.csv",np.transpose(X), delimiter=" ")
np.savetxt("I.csv",np.transpose(IL), delimiter=" ")

fig = plt.figure()
plt.subplots_adjust(hspace=1.0)
ax1 = fig.add_subplot(132)
ax1.plot(X[1], label = 'CD5 High & IL-7R High', color = 'green')
ax1.plot(X[2], label = 'CD5 High & IL-7R Low', color = 'blue')
ax1.plot(X[3], label = 'CD5 Low & IL-7R High', color = 'red')
ax1.plot(X[4], label = 'CD5 Low & IL-7R Low', color = 'purple')
ax1.legend(bbox_to_anchor=(1.0, 1.0))
ax1.set_xlabel('Time (Hours)')
ax1.set_xticks(xticks)
ax1.set_xticklabels(xlabels)
ax1.set_ylabel('Cells')

ax3 = fig.add_subplot(133)
ax3.plot((X[1]+X[2])/X[5], label = 'CD5 High', color = 'blue')
ax3.plot((X[3]+X[4])/X[5], label = 'CD5 Low', color = 'red')
ax3.legend(bbox_to_anchor=(1.0, 1.0))
ax3.set_xlabel('Time (Hours)')
ax3.set_xticks(xticks)
ax3.set_xticklabels(xlabels)
ax3.set_ylabel('Cells')
ax3.set_ylim(0,1)

ax2 = fig.add_subplot(131)
ax2.plot(IL,color = 'blue')
ax2.set_xlabel('Time (Hours)')
ax2.set_xticks(Ixticks)
ax2.set_xticklabels(Ilabels)
ax2.set_ylabel('IL-7 Concentration')
plt.show()
```

APPENDIX C: CODE LISTING FOR POPULATION LEVEL DETERMINISTIC MODEL (SEE SECTION 5.3)

```
# Initial values:
#metabolites
init n12=50
init n22=50
init n21=50
init n11=50
init I=1

# Fixed Model Entities:
param mu1=0.028
param alpha=5
param kap_s=0.8
param mu2=0.017
param lam1=0.083
param kap_p=1.5
param lam2=0.055
param phi1=0.083
param phi2=0.042
param nu=15
param gam1=0.08
param gam2=0.02

# Assignment Model Entities:
n12_c=n12
n22_c=n22
I_c=I
n21_c=n21
n11_c=n11

#Kinetics:
Functio=mu1*n11_c/(1+exp(alpha*(I_c-kap_s)))
Functi=mu1*n12_c/(1+exp(alpha*(I_c-kap_s)))
Functi1=mu2*n21_c/(1+exp(alpha*(I_c-kap_s)))
Functi2=mu2*n22_c/(1+exp(alpha*(I_c-kap_s)))
Functi3=lam1*n11_c/(1+exp(alpha*(kap_p-I_c)))
Functi4=lam2*n21_c/(1+exp(alpha*(kap_p-I_c)))
Functi5=phi1*n12_c
Functi6=phi2*n22_c
Functi7=nu
Functi8=(gam1*(n11_c+n21_c)*I_c+gam2*(n12_c+n22_c)*I_c)

# Equations:
dn12/dt=-Functi+2*Functi3-Functi5
dn22/dt=-Functi2+2*Functi4-Functi6
dI/dt=Functi7-Functi8
dn21/dt=-Functi1-Functi4+Functi6
dn11/dt=-Functio-Functi3+Functi5
done
```